Induced dendritic cells co-expressing GM-CSF/IFN-α/tWT1 priming T and B cells and automated manufacturing to boost GvL

Julia K. Bialek-Waldmann,[1,2] Sabine Domning,[3] Ruth Esser,[4] Wolfgang Glienke,[4] Mira Mertens,[4] Krasimira Aleksandrova,[4] Lubomir Arseniev,[4] Suresh Kumar,[1,2] Andreas Schneider,[1,2] Johannes Koenig,[1,2,5] Sebastian J. Theobald,[1,2,5] Hsin-Chieh Tsay,[2] Angela D.A. Cornelius,[2] Agnes Bonifacius,[6] Britta Eiz-Vesper,[6] Constanca Figueiredo,[6] Dirk Schaudien,[7] Steven R. Talbot,[8] Andre Bleich,[8] Loukia M. Spineli,[9] Constantin von Kaisenberg,[9] Caren Clark,[10] Rainer Blasczyk,[6] Michael Heuser,[1] Arnold Ganser,[1] Ulrike Köhl,[4,11] Farzin Farzaneh,[3] and Renata Stripecke[1,2,5]

[1]Department of Hematology, Hemostasis, Oncology and Stem Cell Transplantation, Hannover Medical School, 30625 Hannover, Germany; [2]Laboratory of Regenerative Immune Therapies Applied, REBIRTH−Research Center for Translational Regenerative Medicine, Hannover Medical School, 30625 Hannover, Germany; [3]Molecular Medicine Group, School of Cancer & Pharmaceutical Sciences, Faculty of Life Sciences & Medicine, Kings College London, London, UK; [4]Institute of Cellular Therapeutics, Hannover Medical School, 30625 Hannover, Germany; [5]German Centre for Infection Research (DZIF), Partner site Hannover, 30625 Hannover, Germany; [6]Institute of Transfusion Medicine and Transplant Engineering, Hannover Medical School, 30625 Hannover, Germany; [7]Fraunhofer Institute for Toxicology and Experimental Medicine, 30625 Hannover, Germany; [8]Institute for Laboratory Animal Science, Hannover Medical School, 30625 Hannover, Germany; [9]Department of Obstetrics, Gynecology and Reproductive Medicine, Hannover Medical School, 30625 Hannover, Germany; [10]Miltenyi Biotec B.V. & Co. KG, 51429 Bergisch Gladbach, Germany; [11]Fraunhofer Institute for Cell Therapy and Immunology IZI and University of Leipzig, 04103 Leipzig, Germany

Acute myeloid leukemia (AML) patients with minimal residual disease and receiving allogeneic hematopoietic stem cell transplantation (HCT) have poor survival. Adoptive administration of dendritic cells (DCs) presenting the Wilms tumor protein 1 (WT1) leukemia-associated antigen can potentially stimulate *de novo* T and B cell development to harness the graft-versus-leukemia (GvL) effect after HCT. We established a simple and fast genetic modification of monocytes for simultaneous lentiviral expression of a truncated WT1 antigen (tWT1), granulocyte macrophage-colony-stimulating factor (GM-CSF), and interferon (IFN)-α, promoting their self-differentiation into potent "induced DCs" (iDCtWT1). A tricistronic integrase-defective lentiviral vector produced under good manufacturing practice (GMP)-like conditions was validated. Transduction of CD14+ monocytes isolated from peripheral blood, cord blood, and leukapheresis material effectively induced their self-differentiation. CD34+ cell-transplanted Nod.Rag.Gamma (NRG)- and Nod.Scid.Gamma (NSG) mice expressing human leukocyte antigen (HLA)-A*0201 (NSG-A2)-immunodeficient mice were immunized with autologous iDCtWT1. Both humanized mouse models showed improved development and maturation of human T and B cells in the absence of adverse effects. Toward clinical use, manufacturing of iDCtWT1 was up scaled and streamlined using the automated CliniMACS Prodigy system. Proof-of-concept clinical-scale runs were feasible, and the 38-h process enabled standardized production and high recovery of a cryopreserved cell product with the expected identity characteristics. These results advocate for clinical trials testing iDCtWT1 to boost GvL and eradicate leukemia.

INTRODUCTION

Acute myeloid leukemia (AML) is a heterogeneous malignant disorder characterized by clonal expansion of myeloid cells.[1] Specific genomic lesions, karyotype anomalies, and clinical variables in AML can be used to predict the event-free survival (EFS) and overall survival (OS).[1] The traditional treatment for AML is induction chemotherapy (with cytarabine and anthracycline), resulting in 65%–75% first complete remission (CR1) for patients ≤60 years, but for patients >60-years old, CR1 is only observed in 40%–60% of patients.[1,2] Patients who show persisting minimal residual disease (MRD) by molecular methods are particularly at high risk of relapse.[3,4] Allogeneic hematopoietic stem cell (HSC) transplantation (allo-HCT) remains the standard clinical care for patients with intermediate- and high-risk AML. For HCT, HSCs and progenitor cells obtained from donors with matching human leukocyte antigens (HLAs) are infused into patients. Upon HCT, the donor cells engraft in the preconditioned host and can eventually reconstitute full

hematopoiesis. For patients >55 years old, a reduced intensity concept (RIC) can be used for immunosuppressive conditioning before HCT to lower the toxicities and side effects. Novel methods based on next-generation sequencing are now applicable to the analyses of AML patients before and after HCT to refine the management of leukemia treatment and eventual relapses.[4] Ultimately, donor-derived T cell reconstitution can be supported by donor lymphocyte infusions (DLIs).[5] HCT plus DLI thus combines purging of the leukemia stem cells with immunotherapeutic graft-versus-leukemia (GvL) effects, resulting in durable survival benefits. Ongoing innovative strategies are being tested to lower the risk of infections and the occurrence of acute and chronic graft-versus-host disease (GvHD).[6] Clinical optimizations reducing morbidities and mortalities after HCT have resulted in increased utilization of HCT as a first-line option for unfavorable- and intermediate-risk patients, including elderly patients.[6,7] DLI can improve survival, but the correlation with GvL is variable and has been associated with increased risk of GvHD. Therefore, novel adjuvant approaches could be developed to enhance the GvL effect and leukemia eradication while keeping GvHD under control. One logical adjuvant approach would be to immunize the patients after HCT against a leukemia-associated antigen (LAA) such as the Wilms tumor protein 1 (WT1). However, this is limited by the prolonged (>6 months) duration of lymphopenia and immunodeficiency after transplantation. Dendritic cells (DCs) are professional antigen-presenting cells (APCs) that capture and process antigens into multiple peptide epitopes and present them efficaciously through HLAs. Thus, the adoptive administration of functional DCs after HCT could potentially help to accelerate the development and priming of lymphocytes for the reconstitution of cellular and humoral responses to combat relapse. We showed that transduction of DC precursors with lentiviral vectors (LVs) expressing granulocyte macrophage-colony-stimulating factor (GM-CSF) and interferon (IFN)-α resulted in *in vivo* self-differentiation into highly viable and immunologically potent "induced DCs" (iDCs).[8,9] We also showed that autologous or donor-derived iDCs co-expressing GM-CSF, interleukin (IL)-4 and truncated WT1 (tWT1) promoted *in vitro* stimulation of WT1-specific memory cytotoxic T lymphocytes (CTLs) capable of killing HLA-matched leukemia cells.[10] Here, we designed a novel tricistronic LV backbone expressing GM-CSF, IFN-α, and tWT1. A batch of integrase-defective (ID)LV particles was produced under good manufacturing practice (GMP)-like (GL) conditions. We show the proof of concept of the feasibility of tWT1, GM-CSF, and IFN-α, co-expression in monocytes after GL-IDLV transduction, promoting their self-differentiation into induced DCs expressing WT1 (iDCtWT1). Two fully humanized mouse models recapitulating human HCT were used to test iDCtWT1 immunizations showing enhanced human T and B cell *de novo* development and maturation. Toward a highly standardized and decentralized production of iDCtWT1, an automated process was established using the CliniMACS Prodigy system. In summary, this work has achieved critical milestones for the future use of iDCtWT1 in the post-HCT setting to accelerate the immune reconstitution, augmenting the GvL effect through cellular and humoral responses to improve the EFS and OS of AML patients.
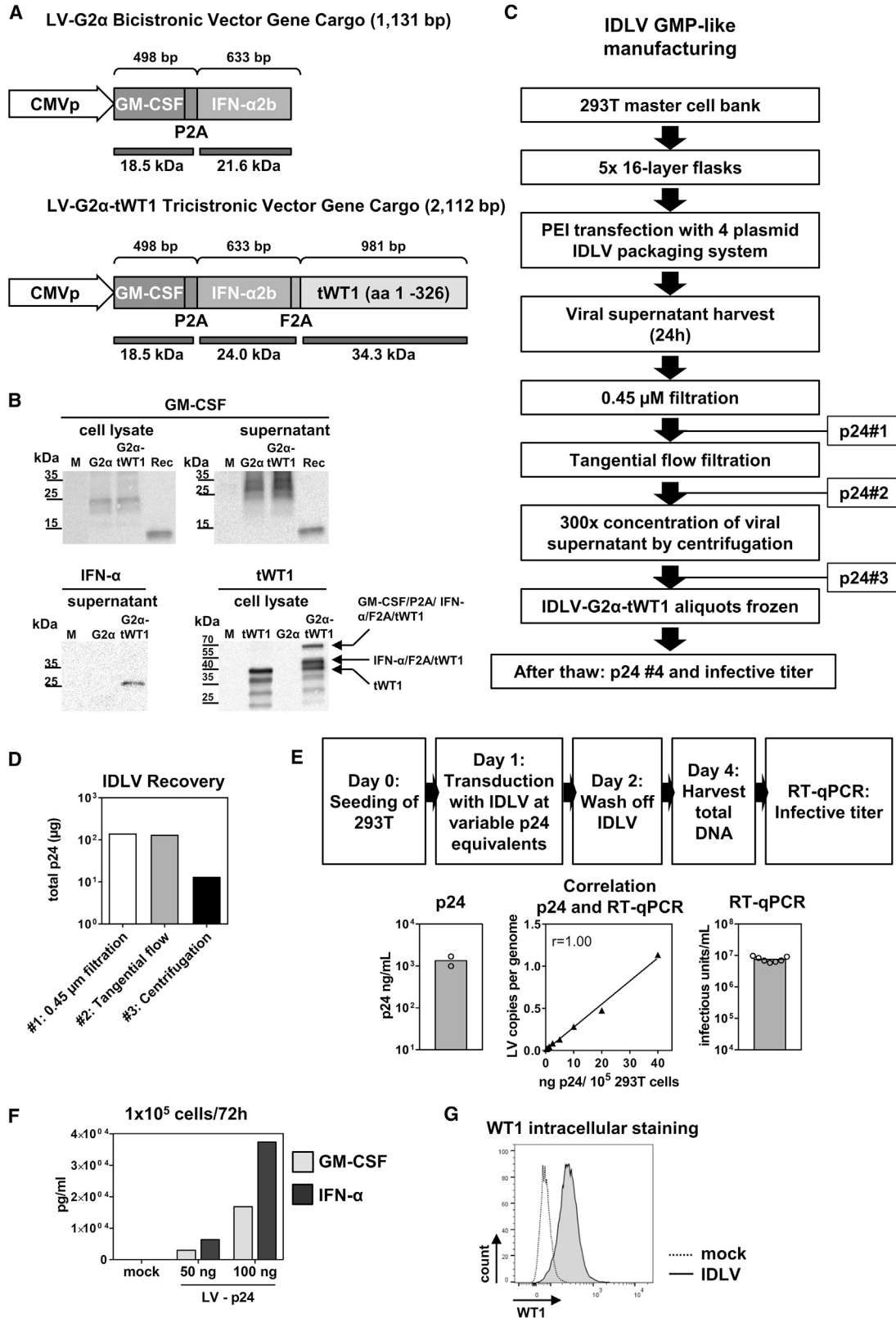
RESULTS

LV-G2α-tWT1 simultaneously expressed secreted GM-CSF and IFN-α and intracellular tWT1

The previously reported bicistronic vector construct co-expressing GM-CSF and IFN-α2b (LV-G2α)[9] was extended into the tricistronic vector LV-G2α-tWT1 after the introduction of the foot-and-mouth disease virus 2A element (F2A) and the sequence encoding tWT1 (amino acids 1–326; Figure 1A). The final "gene cargo" of the resulting tricistronic vector is 2,112 bp. Research-grade (RG) batches of vectors pseudotyped with the vesicular stomatitis virus G glycoprotein (VSV-G) were consistently produced following the third-generation packaging method (with two packaging plasmids, envelope plasmid, and transfer plasmid). 293T cells transduced with integrase-competent (IC)LV co-expressing GM-CSF, IL-4, and tWT1 (LV-G24-tWT1)[10] or ICLV-G2α-tWT1 showed intracellular accumulation of tWT1 expression during 5 days of culture post-transduction (Figure S1). On the other hand, cells transduced with the IDLVs showed a gradual loss of WT1 expression, as the episomal vector was progressively lost upon cell proliferation (Figure S1). Thus, IDLVs carry a lower risk of insertional mutagenesis. The expression of the three transgenes was evaluated by western blot analyses of transduced 293T cells. Comparable levels of GM-CSF were detectable in protein extracts of 293T cells transduced with LV-G2α or LV-G2α-tWT1, prepared either as total cell lysates or as cell supernatants (Figure 1B, upper panels). Secreted IFN-α was detectable for cells transduced with the LV-G2α-tWT1 vector (Figure 1B, lower left panel). The molecular weights observed for GM-CSF-2A and IFN-α-2A were higher than expected, indicating glycosylation. The tWT1 protein was detectable only in total cell lysates as larger fusion protein products (probably translated as a read-through of the polycistron) and as smaller degraded products. In conclusion, LV-G2α-tWT1 expressed simultaneously all of the incorporated transgenes.

GL production and purification of IDLV-G2α-tWT1

We previously reported methods for GL manufacturing of IDLV-G2α-pp65 for generation of iDCpp65 against human cytomegalovirus (HCMV).[11] Here, novel methods were used for IDLV-G2α-tWT1 production. Full sequencing analyses of the LV-G2α-tWT1 backbone vector and the packaging plasmids were performed by a contracted research organization (CRO) (PlasmidFactory, Bielefeld, Germany). Once the plasmid sequences were confirmed, master bacteria cell stocks were established for the production of covalently closed circular (ccc)-grade plasmids. High-purity, ccc-grade plasmids were used for the transfection of 293T cells in multilayer flasks using the polyethylenimine (PEI) method (Figure 1C). Viral supernatants were harvested and subjected to downstream purification (0.45 μm filtration, tangential flow filtration, centrifugation, filling, and storage). The physical viral particle titer was determined by quantification of the HIV-1 p24 core protein by enzyme-linked immunosorbent assay (ELISA) after each processing step. Approximately 10% of the original p24 content was recovered in the final product, indicating the removal of empty vector particles (Figure 1D). After centrifugation and 300-fold concentration, the vector was resuspended in 10 mL volume

A LV-G2α Bicistronic Vector Gene Cargo (1,131 bp)

C IDLV GMP-like manufacturing

B

D

E

F

G WT1 intracellular staining

(legend on next page)

with a titer of 1.34×10^3 ng p24/mL (Figure 1E). The functional titer (infectious units per milliliter) was determined by transduction of 293T cells with serially diluted IDLV-G2α-tWT1 and detection of viral sequences in total cell DNA by quantitative real-time PCR as previously described.[11] The vector copy numbers (VCNs) determined per cell genome were directly correlated with the p24 concentration after serial dilutions of the vector (r = 1.00), and a functional titer of 7.6×10^6 IU/mL was calculated (Figure 1E). GM-CSF and IFN-α were detectable by ELISA in supernatants of 293T cells collected 72 h after transduction with the IDLV-G2α-tWT1 vector ($0.50-1.00 \times 10^2$ ng p24 equivalents) (Figure 1F). Fluorescence-activated cell sorting (FACS) analyses of 293T cells transduced with 1.00×10^2 ng p24 equivalents showed >90% of cells expressing tWT1 (Figure 1G). In conclusion, the GL production of IDLV-G2α-tWT1 was successful, and the vector was functional in transduced 293T cells.

Establishment of iDCtWT1 productions with peripheral blood (PB) and cord blood (CB) after transduction with the GL vector

Monocytes were obtained from fresh PB after gradient centrifugation separation of PB mononuclear cells (PBMCs) and CD14$^+$ magnetic bead isolation (>90% purity). For generation of iDCtWT1, the monocytes were stimulated with recombinant GM-CSF and IL-4 for 8 h, transduced with the GL-IDLV-G2α-tWT1 vector for 16 h, washed, and cryopreserved (see scheme in Figure S2A). As a reference control for transduction, the RG-IDLV-G2α-tWT1 vector produced by calcium phosphate transfection was used at a dose of 2.5×10^3 ng p24 for 5×10^6 cells/mL. After pilot tests, the dose of 1.00×10^2 ng p24 for 5×10^6 cells/mL of GL-IDLV-G2α-tWT1 was shown to be sufficient for the generation of iDCtWT1. PB-iDCtWT1 produced with the purified GL vector showed higher viability at day 7 after thaw (trypan blue analyses) yet lower VCN than cells produced after transduction with higher doses of the RG vector (Figures S2B−S2D). The immunophenotypic characterization of the cells after thawing and 7 days of culture showed high frequencies of viable CD45$^+$/CD11c^{bright} cells. The CD11c^{bright} cells homogenously expressed DC functional markers on the cell surface: the HLA class II molecule HLA-DR, the co-stimulatory molecule CD86, and the DC activation and maturation marker CD83 (Figures S2E and S2G). The viability analyzed by FACS was higher for cells generated with GL than RG vector (Figure S2F). The levels of GM-CSF, IFN-α,

and other DC-endogenous cytokines detectable in iDCtWT1cell supernatants collected on day 7 of culture were similar for the two vectors used (Figures S2H−S2J). Therefore, the GL vector was validated for generation of iDCtWT1 with the expected immunologic properties.
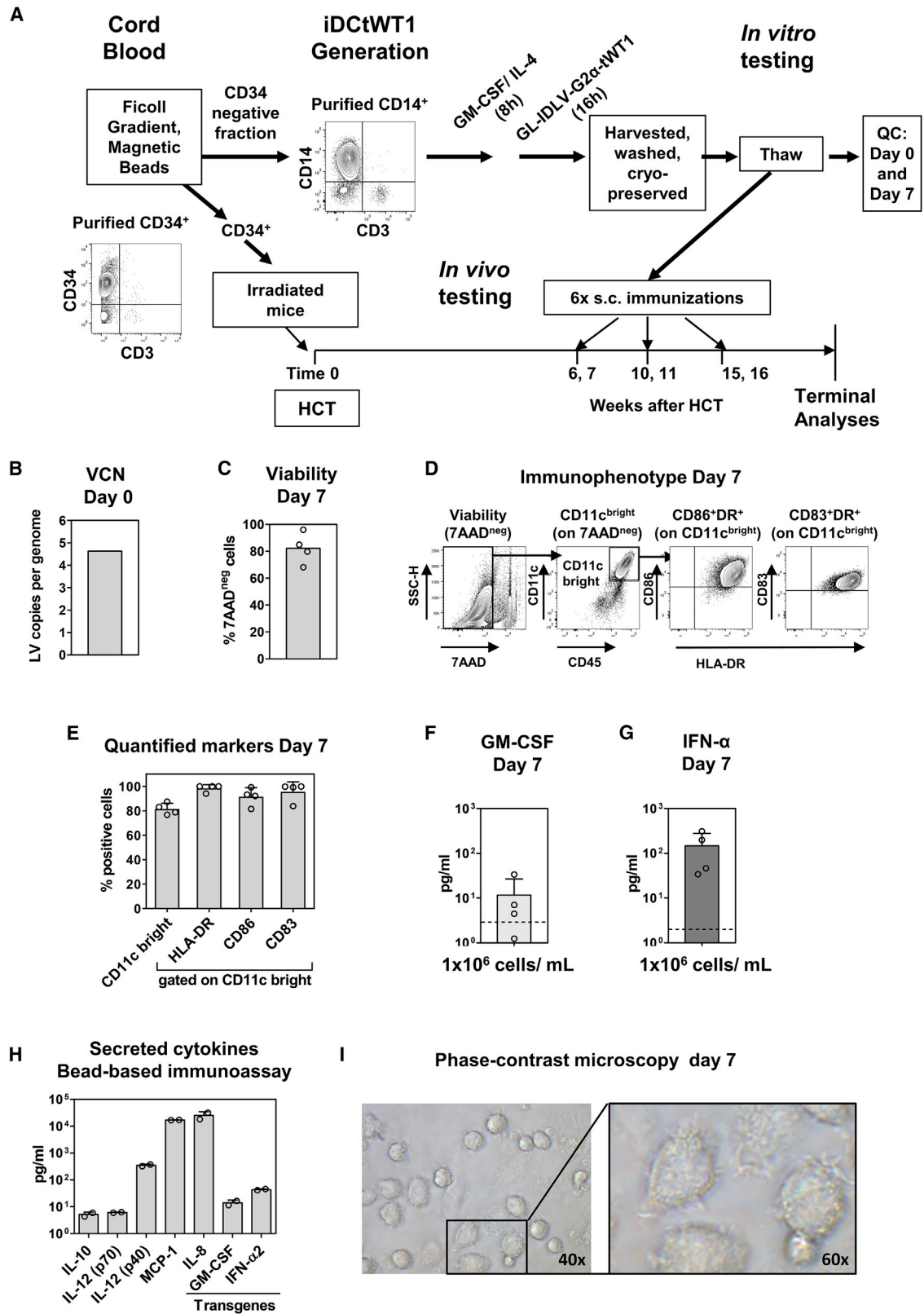
CB is an important alternative stem cell source for HCT of pediatric patients. Thus, we evaluated whether cryopreserved CB could be used for iDCtWT1 generation. Monocytes isolated from the CD34 negative (CD34^{neg}) fraction were transduced with GL-IDLV-G2α-tWT1 and cryopreserved. After thawing, they were used for in vitro quality control (QC) analyses or for in vivo testing in mice transplanted with CD34$^+$ cells isolated from the same CB donor (Figure 2A). For QC, cells were thawed and cultured for 7 days in vitro. On day 0 after thaw, CB-iDCtWT1 contained a VCN of approximately 5 (Figure 2B). CB-iDCtWT1 maintained in culture for 7 days showed high viability (>80% 7-AAD-negative cells) and high frequencies of homogeneous DC populations within the viable cells (Figures 2C−2E). Analyses of cell supernatants by ELISA confirmed the secretion of GM-CSF (average 1×10^1 pg/mL) and IFN-α (average 1×10^2 pg/mL) (Figures 2F and 2G). Bead-array immunoassay analyses detected several cytokines such as IL-10 (average 5×10^0 pg/mL), IL-12/p70 (average 6×10^0 pg/mL), IL-12/p40 (average 3×10^2 pg/mL), MCP-1 (average 2×10^4 pg/mL), and IL-8 (average 2×10^4 pg/mL), indicating an unbiased cytokine composition for activation of both T helper type 1 (Th1) and 2 (Th2) cells (Figure 2H). Microscopic observation on day 7 showed differentiated DCs with the prototypical morphology and presence of dendrites (Figure 2I). In conclusion, CB-CD14$^+$ monocytes transduced with GL-IDLV-G2α-tWT1 generated viable iDCtWT1.

CB-iDCtWT1 applied to Nod.Rag.Gamma (NRG) mice after CD34$^+$ CB-HCT promotes de novo development and maturation of human B and T cells

Fully humanized mouse models are emerging for testing the potency, immune effects, and safety of human-specific immunotherapies.[12] We have previously demonstrated that irradiated NRG mice transplanted with CB CD34$^+$ cells and immunized with iDCs co-expressing the HCMV antigens pp65 or gB antigens showed accelerated development of human mature B and T cells, antigen-specific

---

Figure 1. Design, validation, and GMP-like (GL) production of integrase-defective lentiviral vector (IDLV)-G2α-truncated WT1 (tWT1)

(A) Schematic representation of RRL-derived third-generation LVs containing the CMV promoter. LV-G2α co-expresses human GM-CSF/P2A/IFN-α2b. LV-G2α-tWT1 co-expresses human GM-CSF/P2A/IFN-α2b/F2A linked in-frame to a human tWT1 transgene (tWT1$_{1-326}$) lacking the DNA-binding domain. The sizes of the transgenes are indicated in base pairs, and the expected molecular weights are indicated in kilodaltons. (B) Western blot analyses comparing 293T cells non-transduced mock (M) or transduced with the vectors. Upper panels: analyses of GM-CSF detection in the cell lysate (left) or supernatants (right) comparing mock, LV-G2α-transduced, LV-G2α-tWT1-transduced, and recombinant (Rec) protein as a reference. Lower panel left: analyses of IFN-α2b detection in the supernatant. Lower panel right: analyses of tWT1 detection in cell lysates of cells transduced with the LV-tWT1 and with the LV-G2αtWT1 vector. (C) Production of GL-IDLV-G2α-tWT1 vector. Samples were collected at different steps during the process to measure p24 equivalents by ELISA. (D) Recovery of IDLV-G2α-tWT1 during the process determined by p24 equivalents (total micrograms). (E) Upper panels: 293T cells were transduced with variable amounts of p24 equivalents (nanograms), and the infective titer was obtained by quantitative real-time PCR analyses. Lower left panel: measured p24 titer. Lower middle panel: linear correlation between p24 titer (ng/mL) and numbers of IDLV copies per cell genome. Lower right panel: infective IDLV titer. (F) Concentration of GM-CSF (gray bars) and IFN-α (black bars) in cell supernatants. 293T cells were transduced with GL-IDLV-G2α-tWT1 and 3 days after, seeded at 1×10^5 cells/mL. Supernatants were collected 72 h later, and ELISA was performed. Mock cells showed no detectable cytokines. (G) Flow cytometry detection of WT1 in 293T cells transduced with GL-IDLV-G2α-tWT1 (1.00×10^2 ng/mL p24 equivalent of per 1×10^5 cells) and analyzed 8 days later. Mock cells were used as reference controls.

A

Cord Blood

Ficoll Gradient, Magnetic Beads

Purified CD34+

CD34
CD3

CD34 negative fraction

CD34+

iDCtWT1 Generation

Purified CD14+

CD14
CD3

GM-CSF/ IL-4 (8h)

GL-IDLV-G2α-tWT1 (16h)

Harvested, washed, cryo-preserved

Thaw

In vitro testing

QC: Day 0 and Day 7

Irradiated mice

In vivo testing

6x s.c. immunizations

Time 0

HCT

6, 7   10, 11   15, 16

Weeks after HCT

Terminal Analyses

B

VCN Day 0

LV copies per genome

C

Viability Day 7

% 7AAD^neg cells

D

Immunophenotype Day 7

Viability (7AAD^neg) | CD11c^bright (on 7AAD^neg) | CD86+DR+ (on CD11c^bright) | CD83+DR+ (on CD11c^bright)

SSC-H
7AAD
CD11c
CD45
CD86
HLA-DR
CD83
HLA-DR

E

Quantified markers Day 7

% positive cells

CD11c bright | HLA-DR | CD86 | CD83

gated on CD11c bright

F

GM-CSF Day 7

pg/ml

1×10^6 cells/ mL

G

IFN-α Day 7

pg/ml

1×10^6 cells/ mL

H

Secreted cytokines Bead-based immunoassay

pg/ml

IL-10 | IL-12 (p70) | IL-12 (p40) | MCP-1 | IL-8 | GM-CSF | IFN-α2

Transgenes

I

Phase-contrast microscopy day 7

40x   60x

(legend on next page)

humoral and cellular responses, and broad B cell receptor (BCR) and T cell receptor (TCR) repertoires.[9,13,14] Despite these accelerated immune reconstitutions, no side effects such as acute xenograft GvHD were observed.[14,15] Taking into account that pp65 and gB are viral antigens, here, we explored if iDCs expressing the autoantigen tWT1 could also promote de novo human T and B cell development without causing GvHD. After irradiation and HCT, humanized NRG (huNRG) mice were immunized with cryopreserved CB-iDCtWT1 cells autologous to the CD34^{+} HSCs. The mice were immunized 6 times subcutaneously (s.c.) from week 7 to 16 after HCT (Figure 3A). The experiments were performed as independent duplicates. Only female mice were used for HCT and immunizations, as they showed in our hands more consistent human hematopoietic reconstitution and more robust immune responses.[13] Mice did not show any clinical signs of acute GvHD until the final analysis in week 25 post-HCT (Figure S4A), although two mice immunized with iDCtWT1 showed slight weight losses and skin rashes and were humanely and prematurely terminated due to ethical restrictions. Control mice receiving phosphate-buffered saline (PBS; n = 8) injections and mice immunized with iDCtWT1 (n = 9) showed comparable, persistent, high levels of human CD45^{+} (huCD45^{+}) cells in PB lymphocytes (PBLs) over time, with minor fluctuations (average 43%; Figure 3B; see FACS gating strategies of human lymphocytes in Figure S3A). Within huCD45^{+} cells in PBLs, slightly higher frequencies of CD20^{+}/immunoglobulin G (IgG)[+] B cells and CD4^{+} T cells could be observed over time in mice immunized with iDCtWT1 (Figure 3B). After euthanasia, the lymph nodes were counted, showing a modest increase in numbers for mice immunized with iDCtWT1 (Figure S4B). Analyses of human cytokines detectable in plasma showed that the level of human IFN-γ was significantly higher in the control group (p < 0.05), and the levels of other cytokines were also higher in control mice (IL-1β, IL-2, IL-8, IL-12(p70), and IFN-α). Since IFN-γ is a relevant pro-inflammatory cytokine associated with skin pathologies in the huNRG HCT model[15] and was associated with graft failure in allo-HCT of pediatric patients,[16] these results indicated that iDCtWT1 immunizations may have an anti-inflammatory effect in the HCT model. The levels of human Igs in plasma showed that, with exception of IgG1 and IgG4, all other Igs were increased approximately to 2-fold after iDCtWT1 immunization (Figure 3D; Table 1). This correlated with an overall 2-fold increase in the numbers of CD19^{+}/IgG^{+} and CD19^{+}/IgA^{+} class-switched human B cells detectable by FACS in the spleen of immunized mice (Figure 3E). Immunization was associated with an 1.6-fold increase in the total numbers of huCD4^{+} T cells recovered from the spleen with an effector memory (EM) phenotype

(CD62L^{neg}CD45RA^{neg}) (Figure 3F; see gating strategy in Figure S3). A significant increase in the total numbers of CD8^{+} T cells was observed in the spleen of immunized mice (p < 0.01, 2.3-fold; Figure 3G; Table 1). Within CD8^{+} T cells, both EM and terminal effector (TE) subtypes (CD62L^{neg}CD45RA^{pos}) were significantly increased after immunization (p < 0.01; Figure 3G; Table 1). Total numbers of central memory (CM) CD8^{+} T cells in bone marrow (BM) were also significantly increased after immunization (p < 0.05; Table 1).
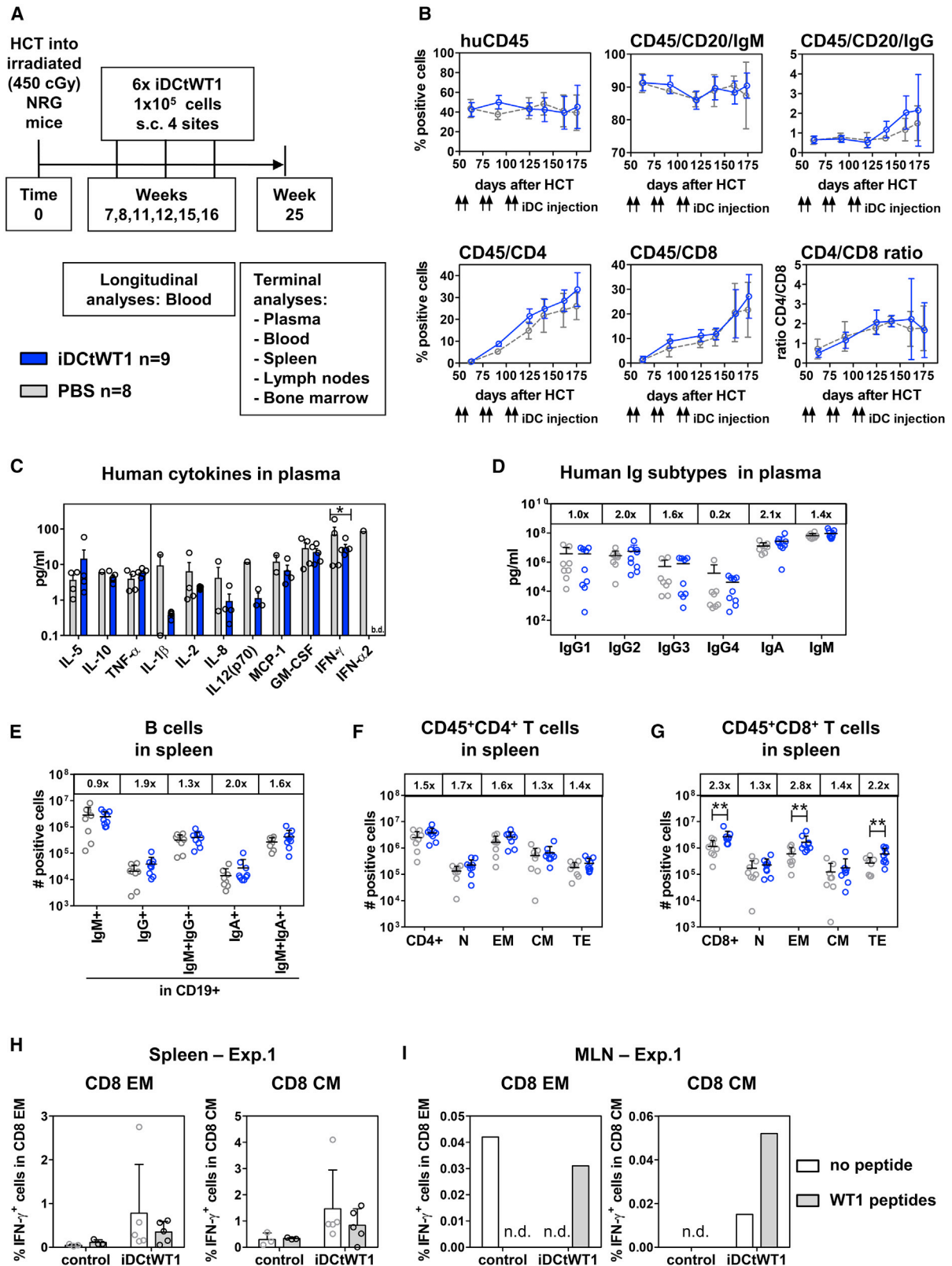
Next, we investigated whether we could detect WT1-specific human CTLs in huNRG mice. Splenocytes recovered from individual mice analyzed in experiment #1 were stimulated with WT1 peptides, and detection of IFN-γ was performed by intracellular staining (ICS) (Figure 3H; see Figure S5 for a description of the ICS assay and FACS gating strategy). Mice immunized with iDCtWT1 showed overall higher frequencies of IFN-γ^{+} EM and CM CD8^{+} T cells than controls (Figure 3H), but the activated T cells in spleen were not WT1 specific, as cells that were not reprimed with peptides also showed higher IFN-γ[+] expression (Figure 3H, white bars). We also performed analyses with pooled lymphocytes recovered from mesenteric lymph nodes (MLNs) of mice. EM and CM CD8^{+} T cells obtained from iDCtWT1-immunized mice and stimulated with WT1 peptides in vitro showed some reactivity, but the frequencies of detectable IFN-γ^{+} cells were very low (less than 0.06%; Figure 3I). Thus, immunization of huNRG with iDCtWT1 promoted the development of class-switched human IgG^{+}/IgA^{+} B cells, EM CD4^{+} Th cells, and CD8^{+} CTLs (Table 1). However, the IFN-γ ICS method used for detection of WT1-specific CTLs in huNRG mice was inconclusive.

Testing iDCtWT1 in humanized Nod.Scid.Gamma (NSG) mice expressing HLA-A*0201 (NSG-A2)

Najima et al.[17] reported that WT1-specific CTLs could be detected by tetramer staining in frequencies of 0.3%–0.6% in tissues of NSG-A2 or for HLA-A*2402 (NSG-24) transplanted with HLA class I-matched HSCs and then immunized with conventional DCs treated with polyinosinic:polycytidylic acid pulsed with WT1 peptides. Therefore, we transplanted NSG-A2 mice with HLA-A*0201-positive CB-CD34^{+} HSCs and immunized them with iDCtWT1 (Figure 4A). The experiments were terminated at 20−21 weeks after HCT, since NSG-A2 mice are more radiation sensitive than NRG mice and showed in our hands sporadic xeno-GvHD. Humanized NSG-A2 (huNSG-A2) mice immunized with iDCtWT1 showed normal human immune reconstitution and higher frequencies of huCD45^{+}/CD4^{+} T cells in PBLs than control mice (Figure 4B). No weight loss

Figure 2. Generation of iDCtWT1 with monocytes isolated from cord blood (CB)
(A) Strategy for generation of iDCtWT1 autologous to the CD34^{+} stem cells used for transplantation of irradiated mice. Cryopreserved iDCtWT1 aliquots were thawed and tested in vitro and then used for immunizations of humanized mice. (B) Vector copy number (VCN) analysis of a representative iDCtWT1 batch after thaw. (C) iDCtWT1 batches were maintained for 7 days in culture, and viability was analyzed (% 7-AAD negative [7-AAD^{neg}]). (D) Representative flow cytometry analyses of thawed iDCtWT1 maintained for 7 days in culture: viability (7-AAD^{neg}), CD45^{+}/CD11c^{bright}, HLA-DR^{+}/CD86^{+}, and HLA-DR^{+}/CD83^{+}. (E) Frequency of cells positive for markers. (F–H) GM-CSF and IFN-α concentrations (pg/mL) measured by ELISA (F and G) and IL-10, IL-12(p70), IL-12p40, MCP-1, IL-8, GM-CSF, and IFN-α2 (pg/mL) measured by bead-based immunoassay (H) in supernatants of day 7 iDCtWT1. (I) Phase-contrast microscopy pictures of day 7 iDCtWT1 (taken at 40× magnification). Left panel: field depicting homogeneous culture. Right panel: isolated cells showing morphology. Bar graphs show the mean values obtained for iDCtWT1 batches produced with different CB units (n = 4).

A

HCT into irradiated (450 cGy) NRG mice

6x iDCtWT1 1x10⁵ cells s.c. 4 sites

Time 0 — Weeks 7,8,11,12,15,16 — Week 25

Longitudinal analyses: Blood

Terminal analyses:
- Plasma
- Blood
- Spleen
- Lymph nodes
- Bone marrow

iDCtWT1 n=9
PBS n=8

B huCD45, CD45/CD20/IgM, CD45/CD20/IgG, CD45/CD4, CD45/CD8, CD4/CD8 ratio plots (% positive cells vs days after HCT, iDC injection)

C Human cytokines in plasma (pg/ml): IL-5, IL-10, TNF-α, IL-1β, IL-2, IL-8, IL12(p70), MCP-1, GM-CSF, IFN-γ, IFN-α2 (b.d.)

D Human Ig subtypes in plasma (pg/ml): IgG1 1.0x, IgG2 2.0x, IgG3 1.6x, IgG4 0.2x, IgA 2.1x, IgM 1.4x

E B cells in spleen (# positive cells): IgM+ 0.9x, IgG+ 1.9x, IgM+IgG+ 1.3x, IgA+ 2.0x, IgM+IgA+ 1.6x in CD19+

F CD45⁺CD4⁺ T cells in spleen (# positive cells): CD4+ 1.5x, N 1.7x, EM 1.6x, CM 1.3x, TE 1.4x

G CD45⁺CD8⁺ T cells in spleen (# positive cells): CD8+ 2.3x **, N 1.3x, EM 2.8x **, CM 1.4x, TE 2.2x **

H Spleen – Exp.1: CD8 EM, CD8 CM (% IFN-γ⁺ cells) control, iDCtWT1

I MLN – Exp.1: CD8 EM, CD8 CM (% IFN-γ⁺ cells) control (n.d.), iDCtWT1; no peptide / WT1 peptides

(legend on next page)

or signs of acute xeno-GvHD were observed in control or immunized mice, and the development of lymph nodes was observed in most mice (Figures S6A and S6B). The levels of human IFN-γ in plasma of the control group were significantly higher than in the immunized cohort (Figure 4C). Other inflammatory cytokines were also more elevated in control mice (IL-1β, MCP-1, and IFN-α), confirming that iDCtWT1 immunization provided anti-inflammatory effects. The levels of several Igs in plasma were noticeably increased after immunization: IgG1 (4.1-fold), IgG3 (2.9-fold), IgG4 (3.2-fold), and IgA (2.0-fold) (Figure 4D; Table 1). FACS analyses showed that iDCtWT1 elevated the development of CD19$^+$/IgG$^+$ (1.6-fold) and CD19$^+$/IgA$^+$ (1.4-fold) class-switched B cells in the spleen (Figure 4E). Immunization was associated with a 1.7-fold increase in the numbers of huCD4$^+$ T cells in the spleen, with the EM (p < 0.05) and CM subtypes being the most enhanced (Figure 4F; Table 1). The total numbers of CD8$^+$ T cells were 1.8-fold higher in the immunized group with a 2.0-fold increase for the EM subtype (Figure 4G). However, analyses of WT1-specific IFN-γ$^+$ CD8$^+$ T cells after in vitro repriming with peptides and ICS showed very low frequencies and inconsistent results (Figures 4H and 4I). In summary, immunization of huNSG-A2 mice with iDCtWT1 confirmed the superior development and maturation of human IgG$^+$/IgA$^+$ B cells, CD4$^+$, and CD8$^+$ EM T cells (Table 1). However, we could not reliably detect WT1-specific CTLs using the IFN-γ ICS method in this partially HLA class I-matched humanized mouse model.

GMP-compatible manufacturing of iDCtWT1 cells in the automated CliniMACS Prodigy cell-processing device

One major advantage of iDCtWT1 is the simple manufacturing of the cell product enabling automatization. Thus, we exemplarily performed two GMP-compatible establishment runs of iDCtWT1 generation using an adaptation of the T cell transduction (TCT) process established for the production of chimeric antigen receptor (CAR)-T cells using the CliniMACS Prodigy system.[18] After collection of the leukapheresis material, the 38-h automated process started with immune magnetic positive selection of CD14$^+$ cells, followed by media exchange, cytokine stimulation, and transduction with RG-IDLV (run 1) or GL-IDLV (run 2) (Figure 5A). The cells were washed three times to remove excess vector, and the cell product was formulated in resuspension buffer, aliquoted, and cryopreserved. QC analyses of identity (cell counts, viability, cell composition) were carried out during the process and for the final product. After cryopreservation, the final product was thawed for characterization of potency on day 0 and after 7 days of in vitro culture (Figure 5A). The frequency of CD14$^+$ cells in the leukapheresis product was approximately 15% (Figure 5B; see gating strategy in Figure S7). Approximately 44% of the volume of the collected leukapheresis material was applied to the apparatus for automated cell selection (total 5.81 × 10^9 cells for run 1 and 8.12 × 10^9 cells for run 2) (Table 2). For runs 1 and 2, the CD14$^+$ target cells were selected, reaching a recovery of 68.7% and 37.6% and a total number of 6.77 × 10^8 and 3.98 × 10^8 cells, respectively. The CD45$^+$CD14$^+$ purity was 98.09% for run 1 and 94.69% for run 2, and only residual CD3$^+$ T cells (0.92% and 1.09% for runs 1 and 2, respectively), residual CD19$^+$ B cells (0.55% and 3.91% for runs 1 and 2, respectively), very few CD56$^+$ natural killer (NK) cells (0.01% for both runs 1 and 2), and no CD34$^+$ HSCs were detectable (Table 2; Figure 5C). Viability after CD14$^+$ cell selection was >95% in both runs (Figure 5E).

After the CD14$^+$ cell selection, a media exchange for culture set-up was performed, and stimulation with GM-CSF and IL-4 was carried out for 6 h. The cells were transduced overnight for 16 h: (1) 1.5 × 10^8 cells were transduced with RG-IDLV using a dose of 2.5 × 10^3 ng p24 equivalents of vector for 5 × 10^6 cells, and (2) 2.0 × 10^8 cells were transduced with GL-IDLV using a dose of 1.0 × 10^2 ng p24 equivalents of vector for 5 × 10^6 cells. The next day, the cells were washed and harvested. The cell composition of the final product showed a CD14$^+$ purity of 88.7% for RG-IDLV, 92.0% for GL-IDLV, and only residual impurities of CD3$^+$ and CD19$^+$ cells, and sparse residual CD56$^+$ cells and CD34$^+$ cells were detected (Figure 5D). The viability of the final product was 32.5% for RG-IDLV transduction (cells cultured in DendriMACS GMP media) and

Figure 3. In vivo testing of iDCtWT1 immunizations in humanized NRG mice

(A) Scheme of experimental design. CB-CD34$^+$ HSCs were used to transplant irradiated NRG mice. Humanized mice were immunized s.c. on weeks 7, 8, 11, 12, 15, and 16 after HCT with 1 × 10^5 autologous iDCtWT1 (n = 9; blue color code throughout the figure). Control mice were treated with PBS (n = 8; gray color code throughout the figure). Blood analyses were performed longitudinally on weeks 9, 13, 17, 20, and 23 after HCT. The experiments were terminated 25 weeks after HCT. (B) Kinetics of human hematopoiesis in blood: frequencies of human CD45$^+$ (huCD45$^+$) cells, CD45$^+$CD20$^+$IgM$^+$ B cells, CD45$^+$CD20$^+$IgG$^+$ B cells, CD45$^+$CD4$^+$ T cells, and CD45$^+$CD8$^+$ T cells and ratios between CD4$^+$ and CD8$^+$ T cells. Mice immunized with iDCtWT1 are shown as blue solid line, and PBS control mice are shown as gray dotted line. Arrows indicate time points of iDCtWT1 injections. Longitudinal data are shown as mean + 95% confidence interval (CI). (C) Human cytokines detectable in plasma (pg/mL). Mice immunized with iDCtWT1 are shown as blue bars, and PBS control mice are shown as gray bars. A dataset below the detection limit (b.d.) is indicated. Shown are mean + standard deviation (SD). Statistical significance was determined using the Holm-Sidak method, with alpha = 0.05. Significance is indicated as *p < 0.05. (D) Human IgG subtypes 1, 2, 3, and 4, IgA, and IgM detectable in plasma (pg/mL). (E) Total number (#) of single- or double-positive IgM$^+$, IgG$^+$, and IgA$^+$ cells within CD19$^+$ B cells in the spleen of PBS control (gray dots, n = 8) or iDCtWT1-immunized mice (blue dots, n = 9). (F and G) Total number of huCD45$^+$/CD4$^+$ T cells or huCD45$^+$/CD8$^+$ T cells in the spleen, respectively, was enumerated in the spleen of PBS control (gray dots, n = 8) or iDCtWT1-immunized mice (blue dots, n = 9). T cell subtypes are shown as naive (N), effector memory (EM), central memory (CM), or terminal effector (TE). Negative binomial regression analysis was performed for total cell counts. Significances are indicated as *p < 0.05. The SD of the mean is shown. Fold difference of the mean comparing the values obtained for PBS controls and iDCtWT1-immunized mice is indicated in the boxes above the graphs and plots. (H and I) In vitro analyses of T cell reactivity against WT1. (H and I) Splenocytes obtained from single mice (iDCtWT1, n = 5; PBS, n = 5) (H) or pooled cells from mesenteric lymph nodes (MLNs) (I) from the first experiment were analyzed. Cells were cultured with cytokines and loaded with an overlapping WT1 peptide mix (WT1 peptides, gray bars) or were not loaded (no peptide, white bars). Intracellular staining for detection of IFN-γ and surface staining for detection of CD8$^+$ T cell EM and CM subtypes were performed. Not detectable (n.d.) indicates no IFN-γ$^+$ cells.

Table 1. Immune effects of iDCtWT1 immunizations in humanized NRG (huNRG) or NSG-A2 humanized (huNSG-A2) mouse models

| | huNRG | | | | | huNSG-A2 | | | | |
| | PBS control | | iDCtWT1 | | | PBS control | | iDCtWT1 | | |
Biomarker	Mean	SD	Mean	SD	p value or fold difference	Mean	SD	Mean	SD	p value or fold difference
%CD45/CD4 in PBL	27.90	3.47	31.28	8.80	0.064	19.75	10.16	26.26	6.39	0.437
#CD4 in Spl	2.49E+06	1.70E+06	4.09E+06	1.95E+06	0.151	2.53E+06	2.39E+06	4.39E+06	3.92E+06	0.079
#CD4 EM in Spl	1.66E+06	1.17E+06	2.78E+06	1.31E+06	0.745	1.47E+06	1.56E+06	2.71E+06	2.47E+06	0.031[a]
#CD8 in Spl	1.17E+06	7.68E+05	2.64E+06	1.89E+06	0.003[a]	1.55E+06	1.38E+06	2.73E+06	2.90E+06	0.437
#CD8 EM in Spl	6.03E+05	4.51E+05	1.60E+06	1.25E+06	0.002[a]	8.01E+05	8.22E+05	1.63E+06	1.82E+06	0.129
#CD8 TE in Spl	2.69E+05	1.68E+05	5.68E+05	5.68E+05	0.008[a]	1.74E+05	1.06E+05	1.61E+05	1.19E+05	0.504
#CD8 CM in BM	1.19E+04	1.23E+04	2.38E+04	2.09E+04	0.035[a]	4.93E+04	5.18E+04	6.78E+04	7.58E+04	0.775
#Single IgG+ B cells in Spl	2.06E+04	1.43E+04	3.90E+04	3.13E+04	1.9×	4.27E+04	3.89E+04	6.66E+04	6.72E+04	1.6×
#Single IgA+ B cells in Spl	1.41E+04	1.19E+04	2.76E+04	3.05E+04	2.0×[b]	4.72E+04	3.72E+04	6.74E+04	2.86E+04	1.4×
#IgG1 in plasma (pg/mL)	3.70E+06	6.26E+06	3.62E+06	4.33E+06	1.0×	2.68E+06	6.17E+06	1.10E+07	1.04E+07	4.1×[b]
#IgG2 in plasma (pg/mL)	2.76E+06	2.99E+06	5.62E+06	8.92E+06	2.0×[b]	2.36E+06	3.14E+06	2.77E+06	2.89E+06	1.2×
#IgG3 in plasma (pg/mL)	4.97E+05	8.64E+05	7.79E+05	9.20E+05	1.6×	3.39E+05	6.20E+05	9.68E+05	8.63E+05	2.9×[b]
#IgG4 in plasma (pg/mL)	1.73E+05	4.77E+05	4.07E+04	4.57E+04	0.2×	5.54E+03	6.54E+03	1.79E+04	3.02E+04	3.2×[b]
#IgA in plasma (pg/mL)	1.25E+07	8.80E+06	2.67E+07	2.76E+07	2.1×[b]	8.94E+06	8.95E+06	1.78E+07	2.03E+07	2.0×[b]

T cell types (effector memory, EM; terminal effector, TE; central memory, CM) and B cells (expressing immunoglobulin [Ig]A or IgG) recovered from spleen (Spl) or bone marrow (BM) were quantified and displayed as frequencies (%) and total number of cells (#). Igs were measured in plasma (pg/mL). Shown are mean, SD, and p value (for analysis of T cell subsets) or ×-fold difference of mean (for analysis of B cells and Igs), comparing PBS controls and iDCtWT1-immunized mice.
[a]Significant p values ≤0.05.
[b]Values representing >2× increase after immunization.

88.9% for GL-IDLV transduction (cells cultured in TheraPEAK X-VIVO 15 media) (Figure 5E). Correspondingly, 20.7% viable CD14+ cells (0.30 × 10^8 total cells) and 80.1% viable CD14+ cells (1.49 × 10^8 total cells) were recovered after RG-IDLV and GL-IDLV transductions, respectively (Table 2). Measurement of VCN in the final product resulted in 1.4 and 0.4 copies per genome for RG-IDLV and GL-IDLV transductions, respectively (Figure 5F). In conclusion, we successfully established an automated process for iDCtWT1 manufacturing. Transduction with the purified GL-IDLV vector resulted in superior viability of the final CD14+ cell product. The low transduction efficiency obtained with GL-IDLV transduction remains to be improved by increasing the vector to cell dose.

In vitro characterization of iDCtWT1 at days 0 and 7 after thawing

Characterizations of iDCtWT1 products were performed after thawing (on day 0) and on day 7 of culture (Figure 6A). The characterizations included analyses of viability, morphology, VCN, DC phenotype, expression of WT1 mRNA, and cytokine production. *In vivo* testing of iDCtWT1 immune effects was performed in long-term reconstituted huNRG mice (Figure 6A). The recovery of viable cells after thawing measured by trypan blue staining was 95.1% for the cell product transduced with RG-IDLV and 76.1% for GL-IDLV (Figure 6B). Viability analyses after 7 days by 7-AAD staining resulted in approximately 67% viable cells for RG-IDLV and 68% for GL-IDLV transduction (Figure 6B). CD14+ isolated cells maintained in the absence of recombinant GM-CSF and IFN-α showed very few viable cells after 7 days of culture,

whereas iDCtWT1/GL-IDLV cells maintained without cytokines showed abundant viable cells with typical DC morphology, similar to CD14+ cells maintained in medium supplemented with cytokines (Figure 6C). The measured VCN was 0.53 for RG-IDLV and 0.03 for GL-IDLV-transduced cells (Figure 6D). Analyses of iDC immunophenotypic markers showed similar frequencies of cells expressing CD11c, HLA-DR, and CD86, but lower frequencies of cells expressing CD83 were observed for GL-IDLV transduction (Figure 6E). Expression of WT1 mRNA was detectable in different types of iDCtWT1 cultures: PBL/CD14+ cells transduced with RG-IDLV, CB/CD14+ cells transduced with GL-IDLV, leukapheresis product/CD14+ cells transduced with RG-IDLV, and leukapheresis product/CD14+ cells transduced with GL-IDLV. The WT1 mRNA expression levels were within the ranges detectable in the positive control K562-A2 and K562-A2-LV-tWT1 cell lines (the latter is a cell line transduced with LV-tWT1 and overexpressing tWT1 mRNA) (Figure 6F). Analyses of cell supernatants collected on day 7 of culture demonstrated a similar pattern for the accumulation of endogenous and transgenic cytokines, but the levels were 1−2 logs lower for cells transduced with GL-IDLV (Figure 6G). Concluding, CD14+ cells transduced in the automated system showed the expected self-differentiation into iDCtWT1, with the product transduced with GL-IDLV showing higher viability but lower expression of CD83, WT1 mRNA, and secreted cytokines. This suggested that higher doses of GL-IDLV to cells should be tested in the future in order to enhance transduction efficacy for iDCtWT1 generation.
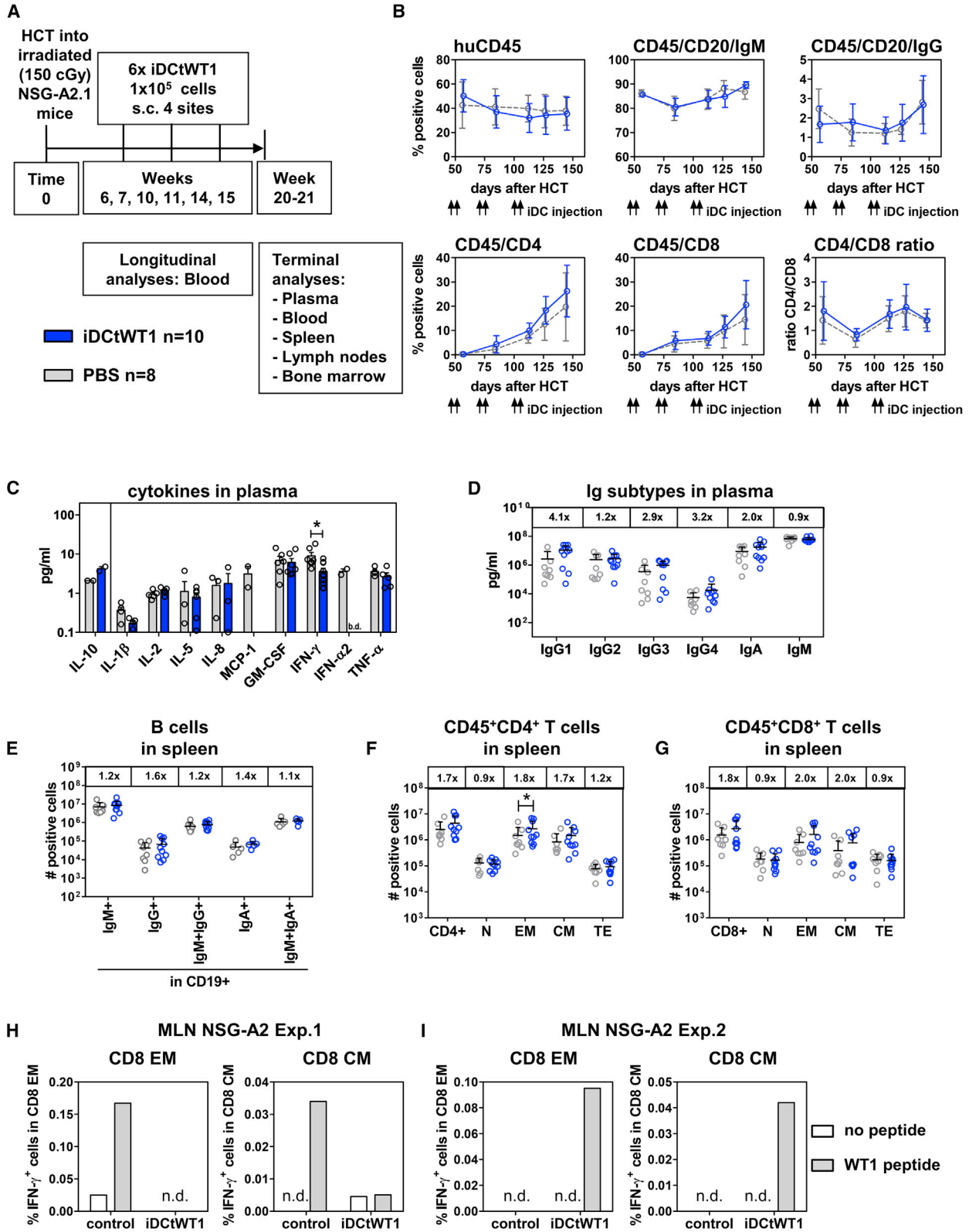
Administration of GL-iDCtWT1 into huNRG and analyses of *in vivo* huCD8^{+} T cell expansion and activation

The guideline on strategies to identify and mitigate risks for first-in-human and early clinical trials with investigational medicinal products of the European Medicines Agency (EMA; https://www.ema.europa.eu/en/strategies-identify-mitigate-risks-first-human-early-clinical-trials-investigational-medicinal) states that if no relevant species exists for non-clinical models, then the use of humanized animals with the human target should be considered. Further, studies conducted in animal models of the intended indication may be used as an acceptable alternative to toxicity studies in normal animals. Therefore, we established a non-clinical humanized mouse model that could be eventually transferred to a CRO to evaluate the *in vivo* safety and potency of iDCtWT1. Pairs of huNRG mice were generated with HSCs from four different CB donors in order to evaluate the variability of results. At 23 weeks after HCT, the mice were injected s.c. with PBS or with a total of 1×10^6 thawed iDCtWT1 generated with GL-IDLV (Figure 6H). The experiment was terminated 10 days later. Immunized mice showed no weight loss. Spleens were collected for histology analyses and FACS. Immunohistochemistry analyses of spleen showed the presence of humanized follicles containing cells intensely staining with the anti-human nuclei (AHN) marker in the white pulp surrounded by the red pulp, with much lesser AHN staining (Figure 6I). Within follicles and surrounding the arteries, most of the human T cells were CD4^{+} T cells with only sparse CD8^{+} T cells (Figure 6I). Immunized mice did not show any histopathological signs of acute GvHD on the skin. GvHD was observed only in one control mouse, as indicated by the presence of apoptotic cells, e.g., in the basal cell layer of the epidermis (Figure S8). FACS analyses showed that the frequencies of huCD45^{+} cells in the spleen remained comparable between the PBS control and iDCtWT1-immunized mice (Figure 6J). However, compared with control mice, immunized mice showed increased frequencies of CD8^{+} T cells (average 2.3-fold increase; Figure 6K) and CD8^{+} TE cells (average 2.0-fold increase; Figure 6L). Thus, this short-term, non-clinical, humanized model showed the ability of iDCtWT1 to prime and stimulate allo-CD8^{+} T cells developed *in vivo* in the animal in the absence of pathological GvHD signs.
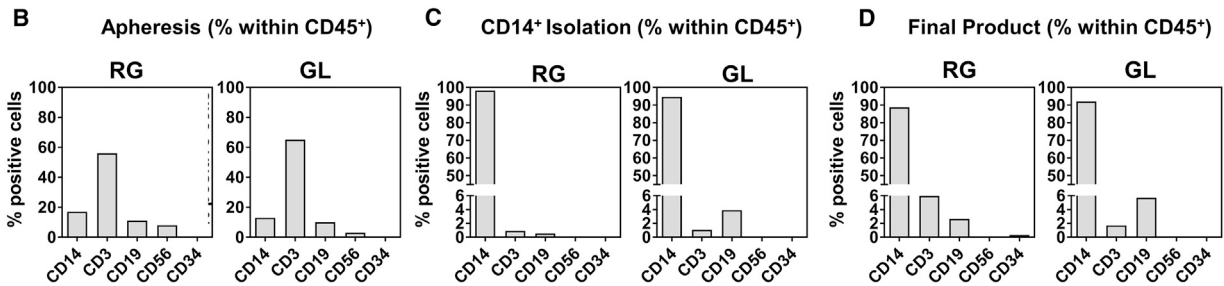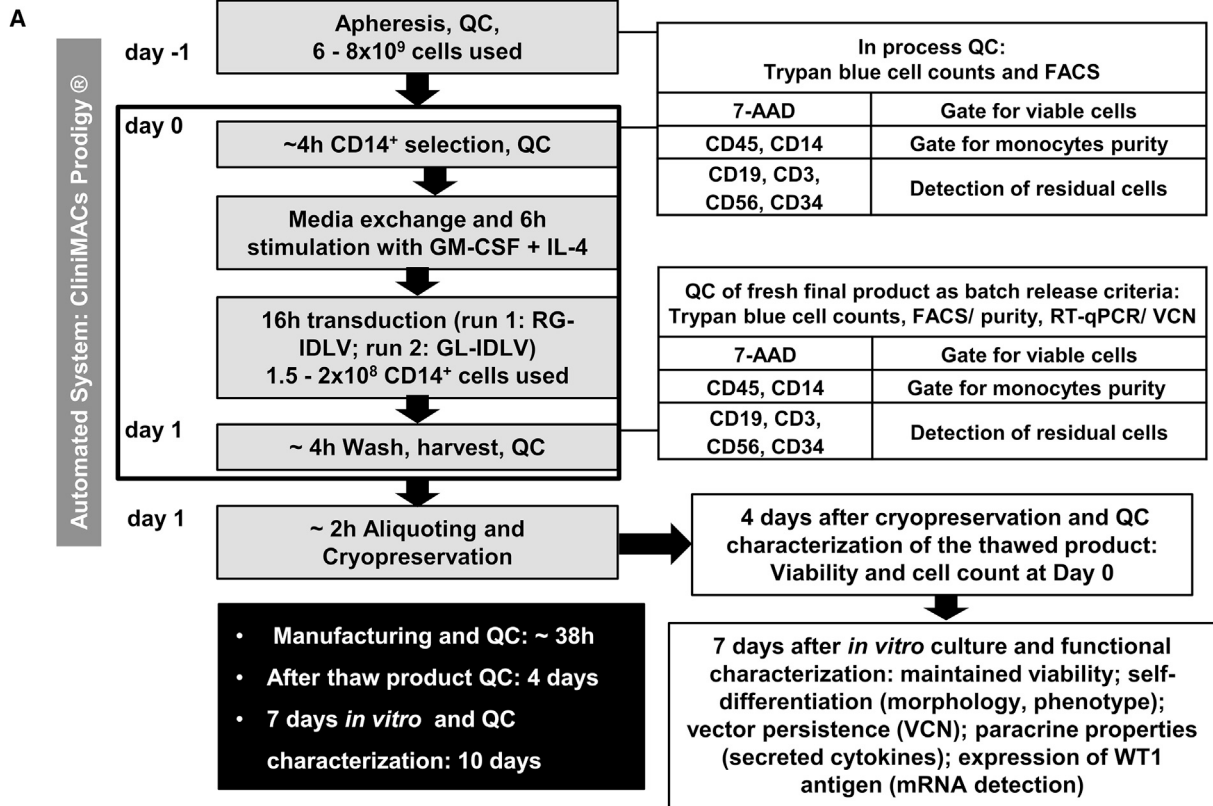
DISCUSSION

Despite that several novel treatment modalities are being tested for MRD[+] AML patients, such as the use of hypomethylating drugs, BCL2 inhibitors, or Hedgehog inhibitors, clinical responses remain transient and variable.[19] Allo-HCT is indicated for patients with intermediate- or adverse-risk AML who are in CR1 and younger than 75 years old.[2] WT1 is both a LAA antigen highly expressed in AML and a biomarker predictive of relapse and therefore an interesting target for AML immunotherapy after HCT.[20,21] Levels of WT1 mRNA detected in PBL by quantitative real-time PCR have been used as a prognostic marker to monitor MRD and to predict relapse after chemotherapy or HCT.[20,21] Several clinical trials exploring WT1 immunogenic peptides to lower AML relapse in CR1 have been performed.[22] Accumulated data from these trials showed higher abundance and functionality of WT1-specific T cells after peptide immunization.[22]
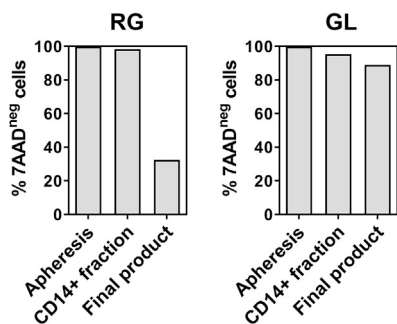
Immunization of post-HCT AML patients is more challenging as the patients are immune compromised. The relevance of appropriate DC levels to induce anti-leukemia immunity in the post-HCT setting has been demonstrated.[23] In fact, we have observed the accumulation of dysfunctional DCs in patients prior to AML relapse.[24] Multiple technologies are currently being developed for the production of adoptive DC vaccines using peptides, vectors, and RNA to enhance antigen loading and presentation.[25] Berneman and colleagues[26] showed in phase I and II clinical trials that vaccination of AML patients in CR1 with *ex vivo*-cultivated autologous DCs electroporated with mRNA expressing full-length or tWT1 was safe and prevented or delayed relapse in up to 43% of patients. OS was correlated with molecular and WT1-specific CD8^{+} CTL responses. Recently, Subklewe and colleagues[27] evaluated autologous DCs transfected with mRNAs (encoding the LAAs WT1 and preferentially expressed antigen in melanoma [PRAME] combined with HCMV-pp65 antigen) and matured with Toll-like receptor agonists. A first-in-human phase I study showed that DC administration to AML patients during remission and at high risk of relapse was feasible and safe and stimulated antigenic T cell responses.

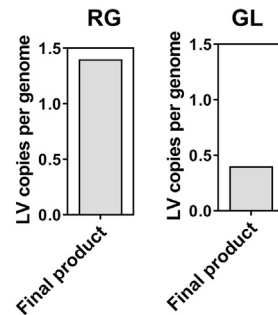**Figure 4. *In vivo* testing of iDCtWT1 immunizations in humanized NSG-A2 mice**

(A) Scheme of experimental design. CB-CD34^{+} HLA-A*02.01-positive HSCs were used to transplant irradiated NSG-A2 mice. Humanized mice were immunized s.c. on weeks 6, 7, 10, 11, 14, and 15 after HCT with iDCtWT1 (n = 10; blue color code throughout the figure). Control mice were treated with PBS (n = 8; gray color code throughout the figure). Blood analyses were performed longitudinally on weeks 8, 12, 16, and 18 after HCT. One experiment was terminated 20 weeks and the other 21 weeks after HCT. (B) Kinetics of human hematopoiesis in blood: frequencies of huCD45^{+} cells, CD45^{+}CD20^{+}IgM^{+} B cells, CD45^{+}CD20^{+}IgG^{+} B cells, CD45^{+}CD4^{+} T cells, and CD45^{+}CD8^{+} T cells and ratios between CD4^{+} and CD8^{+} T cells. Mice immunized with iDCtWT1 are shown as blue solid line, and PBS control mice are shown as gray dotted line. Arrows indicate time points of iDCtWT1 injections. Longitudinal data are shown as mean + 95% CI. (C) Human cytokines detectable in plasma (pg/mL). Mice immunized with iDCtWT1 are shown as blue bars, and PBS control mice are shown as gray bars. Shown are mean + SD. A dataset below the detection limit is indicated. Statistical significance was determined using the Holm-Šidák method, with alpha = 0.05. Significance is indicated *p < 0.05. (D) Human IgG subtypes 1, 2, 3, and 4, IgA, and IgM detectable in plasma (pg/mL). (E) Total number of single- or double-positive IgM^{+}, IgG^{+}, and IgA^{+} cells within CD19^{+} B cells in the spleen of PBS control (gray dots, n = 8) or iDCtWT1-immunized mice (blue dots, n = 9). (F and G) Total number of huCD45^{+}/CD4^{+} T cells or huCD45^{+}/CD8^{+} T cells in the spleen, respectively, was enumerated in the spleen of PBS control (gray dots, n = 8) or iDCtWT1-immunized mice (blue dots, n = 10). T cell subtypes are shown as N, EM, CM, and TE. Negative binomial regression analysis was performed for total cell counts. Significances are indicated as *p < 0.05. The SD of the mean is shown. Fold difference of the mean comparing the values obtained for PBS controls and iDCtWT1-immunized mice is indicated in the boxes above the graphs and plots. (H and I) *In vitro* analyses of T cell reactivity against WT1. For each experiment, T cells recovered from MLNs from the iDCtWT1 group or control were pooled. Cells were cultured with cytokines and loaded with an overlapping WT1 peptide mix (WT1 peptides, gray bars) or were not loaded (no peptide, white bars). Intracellular staining for detection of IFN-γ and surface staining for detection of CD8^{+} T cell EM and CM subtypes were performed. Not detectable indicates no IFN-γ^{+} cells.

A

day -1	Apheresis, QC, 6 - 8x10⁹ cells used
day 0	~4h CD14⁺ selection, QC
	Media exchange and 6h stimulation with GM-CSF + IL-4
	16h transduction (run 1: RG-IDLV; run 2: GL-IDLV) 1.5 - 2x10⁸ CD14⁺ cells used
day 1	~ 4h Wash, harvest, QC
day 1	~ 2h Aliquoting and Cryopreservation

Automated System: CliniMACs Prodigy ®

In process QC:
Trypan blue cell counts and FACS

7-AAD	Gate for viable cells
CD45, CD14	Gate for monocytes purity
CD19, CD3, CD56, CD34	Detection of residual cells

QC of fresh final product as batch release criteria:
Trypan blue cell counts, FACS/ purity, RT-qPCR/ VCN

7-AAD	Gate for viable cells
CD45, CD14	Gate for monocytes purity
CD19, CD3, CD56, CD34	Detection of residual cells

4 days after cryopreservation and QC characterization of the thawed product:
Viability and cell count at Day 0

7 days after *in vitro* culture and functional characterization: maintained viability; self-differentiation (morphology, phenotype); vector persistence (VCN); paracrine properties (secreted cytokines); expression of WT1 antigen (mRNA detection)

- Manufacturing and QC: ~ 38h
- After thaw product QC: 4 days
- 7 days *in vitro* and QC characterization: 10 days

B Apheresis (% within CD45⁺)

C CD14⁺ Isolation (% within CD45⁺)

D Final Product (% within CD45⁺)

E Viability during process

F VCN / Final Product

(legend on next page)

Within the first 100 days after an unrelated donor allo-HCT or HLA-matched sibling transplantation, primary disease and infections account for approximately 50% of deaths (according to the Center for International Blood & Marrow Transplant Research (CIBMTR; https://www.cibmtr.org/ReferenceCenter/SlidesReports/SummarySlides/pages/index.aspx). Because of the delayed immune reconstitution after HCT, MRD+ patients can remain susceptible to opportunistic infections and relapses for months to years. Our goal has been to develop highly viable and potent donor-derived iDCs expressing the tWT1 antigen to exploit the GvL effect in the HCT setting.[28]

Here, iDCtWT1 products were generated with a GL tricistronic IDLV using different sources of CD14+ monocytes (PBL, CB, leukapheresis material) after a short <2-day gene-delivery manipulation. Thus, GMP-compliant iDC production and testing in humanized mice were straightforward, as previously explored for post-HCT iDCpp65 or iDCgB cell therapies against HCMV reactivations.[11] iDCtWT1 immunizations consistently augmented the development and maturation of human T and B cells in two relevant, preclinical, fully humanized mouse models (Table 1). Other groups are also exploring in vivo or ex vivo strategies to redirect and harness DC development and improve their viability and potency.[25] For example, salvage IFN-α treatment applied within 3 months of DLI to MRD+ patients with acute leukemia/myelodysplastic syndromes showed significant improvement in the outcome, and this may be explained by reverting DCs to a functional state.[29] Further, high-risk or relapsed AML patients receiving salvage IFN-α and GM-CSF after HCT and DLI showed in some cases unanticipated long-term remissions.[30] The interpretation of this clinical effect was that IFN-α plus GM-CSF cytokine treatment promoted in vivo differentiation of leukemia progenitor cells toward DCs. It was shown pre-clinically that monocytes modified to express IFN-α reprogrammed the tumor microenvironment and inhibited leukemia in a mouse model.[31] We and others[32] have shown that IFN-α promotes the ex vivo differentiation of mature DCs with migratory capabilities, and therefore, IFN-DCs are actively being exploited in clinical trials for cancer vaccination.

T cells are relevant for GvL responses, as shown by the successful use of DLIs after HCT and the fact that patients treated with T cell-depleted grafts show higher rates of relapse.[33] The regeneration of T cells after HCT can occur via the adoptive transfer of memory T cells or through de novo T cell development in the thymus and other lymphatic tissues. In the humanized mouse models described herein, no adoptive memory T cells were administered. Therefore, the enhanced numbers of EM T cells after iDCtWT1 immunizations

resulted from de novo T cell development and maturation. Najima et al.[17] have reported the detection of HLA*0201-restricted WT1-reactive CTLs by tetramer staining analyses in NSG-A2 using conventional DCs pulsed with WT1 peptides, but we could not reproduce this in NSG-A2 mice immunized with iDCtWT1. In our hands, the direct assessment of the WT1-specific responses in the humanized mice was challenging and inconsistent, due to the following: (1) limited amount of T cells available for analyses recovered from spleen or lymph nodes, (2) the complexities of the human-mouse major histocompatibility complex (MHC) mismatches resulting in suboptimal-positive and -negative selection of TCRs, and (3) low frequencies of WT1-reactive CTLs detectable by the IFN-γ ICS method. These factors may explain why we could not reliably detect WT1-specific CTLs using similar ICS methods that previously resulted in the successful detection of WT1-reactive CD8+ and CD4+ memory T cell responses in the majority of healthy human volunteers.[34] We (R.S. and K.S., unpublished data) and others[35] are currently testing new transgenic mouse strains and developing technologies to match the class II and class I HLAs of human cells with mouse tissues to support CD4+ Th and CD8+ CTL development and immune responses.

Despite the HLA/mouse MHC disparities that can account for the challenging analyses of WT1-specific CTL responses, an interesting observation was that iDCtWT1 stimulated B cell maturation and IgG and IgA class switching. This was not surprising, as we have previously observed similar effects in humanized mice for the similar product iDCgB.[14] Thus, the humoral effects after iDCTWt1 immunization represent a novel immunotherapeutic aspect for enhancement of GvL effects. Indeed, several therapies exploring antibody recognition of AML antigens are underway to promote cytotoxicity against AML,[36] also including immune checkpoint inhibitors (ICIs) and T cells engineered with CARs (CAR-T cells).[37,38]

As discussed above, the manufacturing of DCs modified with mRNAs encoding WT1 for phase I and II clinical trials was feasible, and promising immunological and therapeutic effects against AML were observed.[27,39] Nevertheless, the manufacturing of these ex vivo-cultivated DC vaccines is complex and requires several steps and different types of GMP-grade reagents for antigen loading and maturation. We previously demonstrated feasibility of a 2-day protocol for GL manufacturing of iDCpp65 after CD14+ monocyte selection on CliniMACS and subsequent LV transduction in bags.[11] Here, we were able to advance toward a GL-IDLV and automated cell-manufacturing methods. Tangential flow filtration of GL-IDLV prior to ultracentrifugation was performed to remove empty virus particles. Pilot transduction experiments in the research laboratory showed that 25-fold less

Figure 5. Proof of feasibility of automated iDCtWT1 manufacturing in the CliniMACS Prodigy
(A) Scheme of the process for the production of iDCtWT1 in a closed automated system (gray boxes), QC analyses (white boxes), and estimated time for manufacturing, QC, and characterization (black box). (B–F) Two manufacturing runs were performed comparing transduction with research-grade (RG)-IDLV and GL-IDLV. (B–D) Frequencies of CD14+, CD3+, CD19+, CD56+, and CD34+ cells within CD45+ viable (7-AADneg) cells determined by flow cytometry for analysis of identity and purity in: (B) leukapheresis material, (C) CD14+ fraction after selection, and (D) final product before cryopreservation. (E) Cell viability is defined as percent 7-AADneg cells in leukapheresis material, CD14+ fraction after selection, and final product after transduction with IDLV (before cryopreservation). (F) VCN after transduction with IDLV (final product before cryopreservation).

Table 2. Comparisons between two pilot automated iDCtWT1 manufacturing productions using the CliniMACS Prodigy device

	Input cells ($\times 10^8$)	Purity CD14$^+$ (%)	Isolated CD14$^+$ ($\times 10^8$)	Cells transduced ($\times 10^8$)	IDLV ng p24 equivalents per 5×10^6 cells	Viability in product (%)	Purity CD14$^+$ (%)	Cells in product ($\times 10^8$)	VCN in product
Run 1 RG-IDLV	58.14	98.1	6.77	1.5	2.5×10^3	32.5	88.7	0.30	1.4
Run 2 GL-IDLV	81.17	94.7	3.98	2.0	1.0×10^2	88.9	92.0	1.49	0.4

Run 1: CD14$^+$ cells were transduced with research-grade (RG)-IDLV and cultured in DendriMACS GMP media. Run 2: CD14$^+$ cells were transduced with GMP-like (GL)-IDLV and cultured in TheraPEAK X-VIVO 15 media. VCN, vector copy number.

p24 ng equivalents of the GL-IDLV compared with RG-IDLV yielded higher frequencies of viable-differentiated iDCtWT1 at day 7 (Figure S2). This effect was confirmed in the iDCtWT1 manufacturing runs performed in CliniMACS Prodigy (Figure 5E). This indicated that impurities in the raw RG-IDLV produced toxic effects affecting the cell viability. Yet, lower transduction efficiency measured by VCN and expression of *WT1* mRNA and of CD83 were obtained with iDCtWT1 produced with GL-IDLV (Figures 5F, 6E, and 6F). Therefore, for future optimizations, higher amounts of the purified GL-IDLV remain to be tested in CliniMACS Prodigy to yield simultaneously high viability, high transduction efficiency of monocytes, and high *WT1* mRNA and CD83 expression in the differentiated iDCtWT1 cells.

Although further preclinical optimizations, validations, and analyses will be required, we have set a clear path for translation using a system that allows a decentralized and global production of iDCtWT1 in clinical centers treating high-risk AML patients after HCT see graphical abstract. For clinical development, donors after HSC mobilization and apheresis collection will be asked to undergo a second, short leukapheresis for manufacturing of iDCtWT1 and generation of the cryopreserved cell product. After HCT engraftment is confirmed, and no GvHD is evident, two cycles of iDCtWT1 prime/boost applications will be administered within the first 100 days after HCT. In summary, we have used gene-therapy approaches and advanced automated cell-manufacturing methods to develop the novel iDCtWT1immunotherapeutic product, which can be used as a reprogrammed monocyte vaccine resulting in iDCs. *De novo* T and B cell immune-stimulatory effects and safety aspects of iDCtWT1 could be shown in relevant humanized mouse models. First-in-human clinical trials are currently being proposed to evaluate the effects of iDCtWT1 immunizations after HCT to improve the survival of AML patients.

MATERIALS AND METHODS
Ethics statement
Umbilical CB units were obtained from the mothers in accordance to study protocols approved by Hannover Medical School (MHH) Ethics Review Board under written, informed consent (approval number [no.] 4837). Mice experiments were performed in accordance with European Union (EU) directive 2010/63 and the German Animal Welfare Law and permitted by the Lower Saxony State Office for Consumer Protection and Food Safety (approval no. 33.12-42502-04-16/2347). For the automated GL manufacturing of iDCtWT1, leukapheresis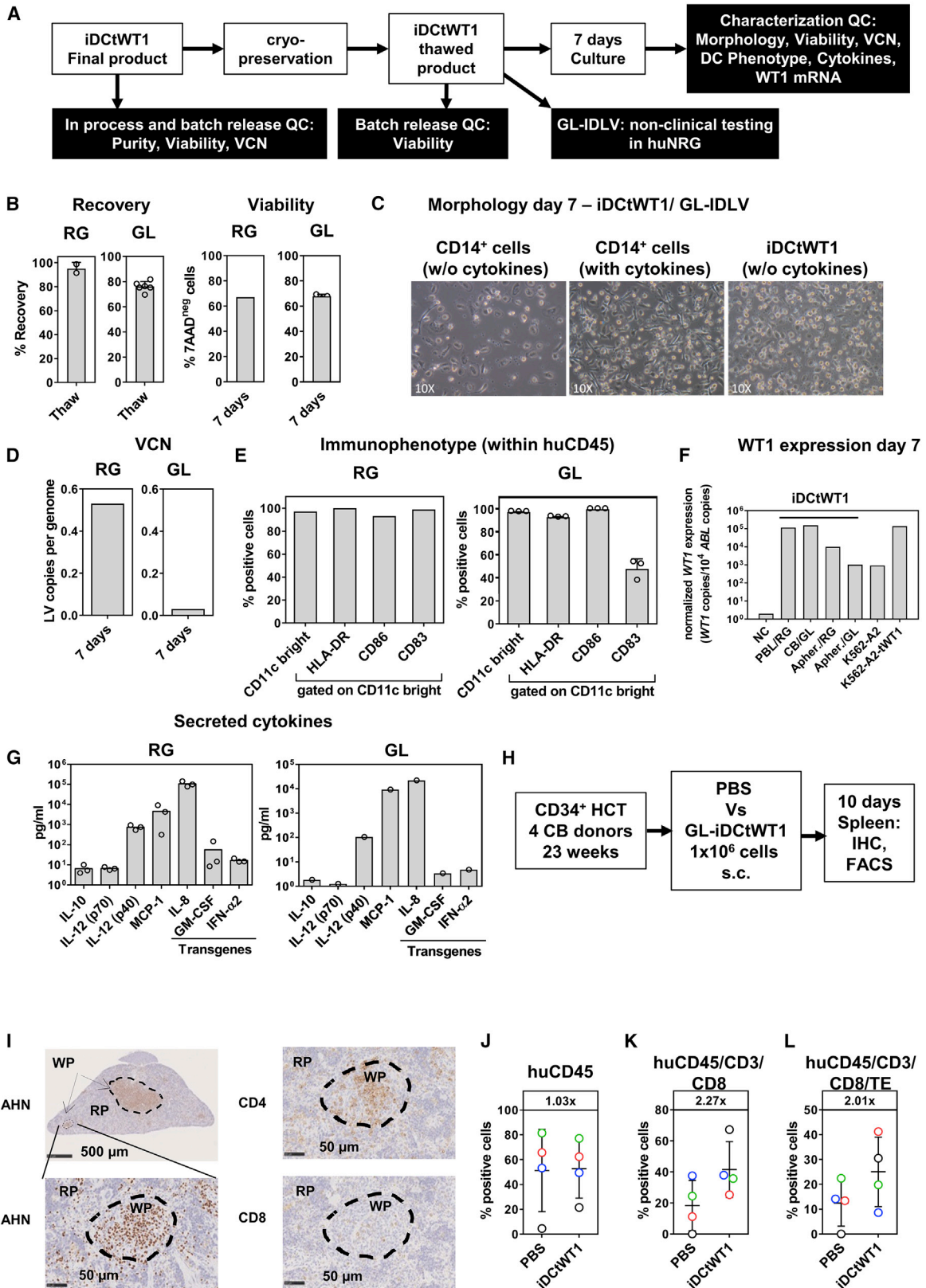 products from healthy donors were obtained from the Institute for Transfusion Medicine of MHH after donors' written, informed consent. According to standard donation requirements, donors had no signs of acute infection and no previous history of blood transfusion. The study was approved by the Ethics Committee of the MHH (protocol no. 4837).

Cell culture and selection of primary cells
HEK293T cells (human embryonic kidney cells; ATCC) were expanded and cultured in Dulbecco's modified Eagle's medium (DMEM) (Thermo Fisher Scientific, Waltham, MA, USA) containing 10% fetal bovine serum (FBS; HyClone, Logan, UT, USA) and 1% penicillin/streptomycin (Merck Millipore, Billerica, MA, USA) at 37°C with 5% CO_2. PBMCs were isolated by Ficoll gradient centrifugation as described previously.[13] Immune magnetic separation was used to isolate CD14$^+$ and CD34$^+$ cells (Miltenyi Biotec, Bergisch-Gladbach, Germany) as described.[13]

LV construction and production
The self-inactivating (SIN) LV expressing GM-CSF, IFN-α2b, and tWT1 (G2α-tWT1), interspaced with a porcine teschovirus-1 2A element (P2A) and F2A, was constructed by overlapping PCR as previously described.[10] Transient transfection of 293T cells was performed with the transfer plasmid vector LV-G2α-tWT1 and the packaging plasmids: pCDNA3.g/p.4xCTE encoding the D64V mutation in the integrase gene, pRSV/Rev expressing Rev, and the pMD.G plasmid encoding for the VSV-G. Transfection was performed essentially as described[9] and later adapted to the PEI transfection method.[40] All plasmids were produced at ccc-grade quality (ccc and supercoiled, enzyme free, devoid of any substances of animal origin, endotoxin free, and certified for purity) and fully sequenced by PlasmidFactory (Bielefeld, Germany). IDLV-G2α-tWT1 was produced under GL conditions after several adaptations of the standard operation procedures previously established at Cell and Gene Therapy at King's College London.[41] Briefly, multi-layer culture flasks were seeded with 293T cells and cultured to sub-confluent optimal density in DMEM. PEI transfection was performed with the transfer and packaging plasmids. 24 h after transfection, medium change was performed. The supernatant containing virus was harvested after 24 h. The virus supernatant was clarified through 0.45 μm filters and processed by tangential flow filtration and subjected to high-speed centrifugation. The virus pellet was resuspended in PBS. A 300×-fold volume reduction was achieved from bulk harvest to final concentration. The PBS formulated final concentrated virus suspension was filled in 100 μL per vial aliquots and stored at −80°C.

A

iDCtWT1 Final product → cryo-preservation → iDCtWT1 thawed product → 7 days Culture → **Characterization QC: Morphology, Viability, VCN, DC Phenotype, Cytokines, WT1 mRNA**

In process and batch release QC: Purity, Viability, VCN

Batch release QC: Viability

GL-IDLV: non-clinical testing in huNRG

B Recovery / Viability

C Morphology day 7 – iDCtWT1/ GL-IDLV

CD14⁺ cells (w/o cytokines) / CD14⁺ cells (with cytokines) / iDCtWT1 (w/o cytokines)

D VCN

E Immunophenotype (within huCD45)

F WT1 expression day 7

G Secreted cytokines — RG / GL

H

CD34⁺ HCT 4 CB donors 23 weeks → PBS Vs GL-iDCtWT1 1×10⁶ cells s.c. → 10 days Spleen: IHC, FACS

I / **J** huCD45 — 1.03x / **K** huCD45/CD3/CD8 — 2.27x / **L** huCD45/CD3/CD8/TE — 2.01x

(legend on next page)

Western blot analyses to confirm expression of the transgenes

1×10^5 293T cells were transduced with 1 μg p24 equivalent of RG-IDLV-G2α-tWT1, IDLV-G2α (expressing GM-CSF and IFN-α2b), or LV-tWT1 (expressing tWT1), produced by standard methods as described previously[42] and harvested 3 days later. Culture supernatants and cell lysates were separated based on the molecular weight by sodium dodecyl sulfate-polyacrylamide gel electrophoresis (SDS-PAGE; AnykD gel, Bio-Rad Laboratories). The proteins were transferred to nitrocellulose membranes using the Mini-PROTEAN Tetra electrophoresis system (Bio-Rad Laboratories). Immunodetection was performed with the following primary antibodies: rabbit anti-human GM-CSF (catalog no. 500-P33; PeproTech, Cranbury, NJ, USA), mouse anti-human IFN-α (catalog no. 3110; Cell Signaling Technology, Danvers, MA, USA), and mouse anti-human-WT1 (catalog no. sc-7385; Santa Cruz Biotechnology, Dallas, TX, USA). After incubation with the secondary antibodies coupled to horseradish peroxidase, the proteins were detected using the SuperSignal West Pico Chemiluminescent Substrate Kit (Thermo Fisher Scientific, Darmstadt, Germany) according to the manufacturer's instructions.

Intracellular detection of WT1 by flow cytometry

1×10^5 293T cells were transduced with 1×10^2 ng p24 equivalent of GL-IDLV-G2α-tWT1 and harvested 8 days after transduction. Cells were permeabilized and fixed with Cytofix/Cytoperm solution (Becton Dickinson [BD], Heidelberg, Germany) according to the manufacturer's instructions, followed by incubation with monoclonal mouse anti-WT1 and a secondary antibody (antibodies used are listed in Table S1). Cells were then washed with BD Perm/Wash solution (BD) and analyzed by flow cytometry.

Determination of IDLV-G2α-tWT1 particle content by p24 measurement

Physical titers of the vectors produced were determined by quantifying the p24 HIV-1 core protein by ELISA (QuickTiter HIV Lentivirus Quantitation Kit, BioCat, Heidelberg, Germany, for RG-IDLV; and

HIV-1 p24 Antigen ELISA, ZeptoMetrix, Buffalo, NY, USA, for GL-IDLV) according to the manufacturer's instructions.

Determination of LV titer by quantitative real-time PCR and VCN analysis

Genomic DNA was isolated from 1×10^6 transduced or non-transduced cells ($-20°C$ frozen cell pellets) with the QIAamp DNA Blood Mini Kit (QIAGEN, Hilden, Germany) according to the manufacturer's protocol. Standard curve quantification was performed with five serial dilutions ($1 \times 10^6 - 1 \times 10^2$ copies) of the PTBP2-WPRE single-copy gene-containing plasmid "pQPCR-Stdx4."[43] Specific primers for WPRE (forward: 5′-GAGGAGTTGTGGCCCGTTGT-3′, reverse: 5′-TGACAGGTGGTGGCAATGCC-3′, probe: 5′-CTGT GTTTGCTGACGCAAC-3′ (5′-FAM-3′-BHQ1); and PTBP2 (forward: 5′-TCTCCATTCCCTATGTTCATGC-3′, reverse: 5′-GTTC CCGCAGAATGGTGAGGTG-3′, probe 5′-ATGTTCCTCGGAC CAACTTG-3′ (5′-JOE-3′-BHQ1) (BioSpring, Frankfurt am Main, Germany)[43] were used with the TaqMan Fast Advanced Master Mix (Thermo Fisher Scientific) and the StepOnePlus Real-Time PCR Detection System (Applied Biosystems, Darmstadt, Germany). Cycling conditions were $95°C$, 2 min (initial step); $95°C$, 1 s; and $58°C$, 5 s (data accumulation), with 40 cycles. All samples were tested in triplicate, and negative controls were included to monitor sample cross-contamination. The in-house established control cell line 293T-bright3 (containing three WPRE copies per genome) served as an internal control. The quantitative real-time PCR was performed according to the MIQE guidelines to facilitate the standardization of the qPCR results.[44]

Generation of iDCtWT1 and QC

The same CB unit used as a source of CD34$^+$ cells for mouse HCT was used for iDCtWT1 production. For the generation of iDCtWT1, CD14$^+$ monocytes were isolated from the CD34$^-$ fraction using immune magnetic beads (Miltenyi Biotec). After isolation, monocytes were pre-conditioned with recombinant human GM-CSF and IL-4 (both 50 ng/mL; Miltenyi Biotec) for 8 h at $37°C$ in X-VIVO 15

Figure 6. Characterization of iDCtWT1 manufactured in CliniMACS Prodigy

(A) Scheme of the process for characterization of iDCtWT1. Viability, purity, and VCN were assessed in the final product before cryopreservation. For characterization purposes after cryopreservation and thaw, viability was re-assessed, and cells were cultured *in vitro* without the addition of cytokines. After 7 days of culture, morphology, viability, DC phenotype by flow cytometry, and *WT1* mRNA expression by quantitative real-time PCR were assessed. Additionally, iDCtWT1 produced with GL-LV were used for *in vivo* testing in fully humanized mice. (B) Left panels: recovery measured by trypan blue staining; right panels: cell viability measure by 7-AAD^{neg} staining by FACS. (C) Morphology of iDCtWT1 produced with GL-LV after 7 days of *in vitro* culture without cytokines. CD14$^+$ cells from the same manufacturing run were cultivated with and without cytokines as controls. (D) VCN determined by quantitative real-time PCR after 7 days of *in vitro* culture. (E) Flow cytometry analysis to show the phenotype of iDCtWT1 after 7 days of culture: viable (7-AAD^{neg}) cells, CD11c^{bright} gated on live cells (7-AAD^{neg} population), and HLA-DR$^+$ in combination with CD83$^+$ and CD86$^+$. (F) *WT1* mRNA expression determined by quantitative real-time PCR. iDCtWT1 was produced from peripheral blood (PB) with RG-IDLV (PBL/RG: 2.5×10^3 ng p24 per 5×10^6 cells), from CB (CB-GL: 1.00×10^2 ng p24 per 5×10^6 cells), or leukapheresis material in the automated CliniMACS Prodigy system (with RG-LV or GL-IDLV). Cells were thawed and cultured for 7 days, and RNA was isolated and cDNA synthesized. The K562-A2 cell line and a K562-A2-tWT1 line served as references. CD14$^+$ cells cultured for 7 days with cytokines served as negative control (NC). The expression of WT1 mRNA was detected in relation to the expression of the ABL reference mRNA. (G) Detection of secreted IL-10, IL-12(p70), IL-12p(p40), MCP-1, IL-8, GM-CSF, and IFN-α2 (cells seeded 1×10^6 cells/mL and supernatant harvested 7 days after). Shown is the mean of three independent *in vitro* cultures of the iDCtWT1 final product. (H) Experimental model to evaluate humanized NRG mice immunized s.c. on week 23 after HCT with 1×10^6 thawed GL-iDCtWT1 produced in CliniMACS Prodigy (n = 4; color code indicates different CB units used for HCT). Control mice were treated with PBS after HCTs (n = 4). Mice were sacrificed, and analysis of spleen was performed 10 days after immunizations. (I) Immunohistochemistry analyses of anti-human nuclei (AHN), CD4, and CD8 using spleen of a humanized mouse. Right panels show detectable follicles containing the AHN$^+$ humanized white pulp (WP) within the red pulp (RP). Left upper panel showing staining of CD4$^+$ and left lower panel staining of CD8$^+$ T cells in the WP. (J) Percentage of huCD45$^+$. (K) Percentage of huCD45$^+$/CD3$^+$/CD8$^+$. (L) Percentage of huCD45$^+$/CD3$^+$/CD8$^+$ TE cells in spleen measured by flow cytometric analysis.

serum-free medium (Lonza, Basel, Switzerland). Afterward, media were removed, and GL-IDLV-G2α-tWT1 (100 ng/mL p24 equivalent) plus 5 μg/mL protamine sulfate (Valeant, Duesseldorf, Germany) was added. Transduction was performed for 16 h, and afterward cells were washed extensively with PBS and cryopreserved. For batch release and QC, an aliquot of the batch was thawed, adjusted to 1×10^6 cells/mL, and cultured for 7 days in X-VIVO 15 medium. Immediately after thaw, cells were analyzed for identity and purity (CD45, CD14, CD3, CD19, CD56, and CD34) by flow cytometry. On day 7 after thaw, cells were analyzed for DC differentiation (CD11c, CD83, CD86, and HLA-DR) (the antibodies used are listed in Table S1). GM-CSF and IL-4 were detected by ELISA using cryopreserved supernatants collected on day 7 of cell cultures (Mabtech, Stockholm, Sweden). Samples were thawed on ice, diluted, and measured in duplicates. ELISA plates were analyzed with the SpectraMax 340PC384 plate reader and SoftMax Pro software (Molecular Devices, San Jose, CA, USA). For immunizations, cells were thawed, washed in PBS, counted, adjusted for the cell density, and administered.

HCT and iDCtWT1 immunization

NOD.Cg-*Rag1*^*tm1Mom* *Il2rg*^*tm1Wjl*/SzJ (NRG) and NOD.Cg-*Mcph1*^*Tg(HLA-A2.1)1Enge* *Prkdc*^*scid* *Il2rg*^*tm1Wjl*/SzJ (NSG-HLA-A2.1; NSG-A2) mice were obtained from The Jackson Laboratory (JAX; Bar Harbor, ME, USA) and bred and maintained under pathogen-free conditions at the Central Animal Facility of MHH. Female mice were used for all experiments because they showed more consistent immune reconstitutions.[13] HCT was performed as previously described.[42] Briefly, 5- to 6-week-old mice were sub-lethally irradiated (NRG: 450 cGy; NSG-A2: 150 cGy) using a [137Cs] column irradiator (Gammacell 3000 Elan; Best Theratronics, Ottawa, Canada). 4 h after irradiation, 2.0×10^5 human CB-CD34$^+$ cells were injected into the tail vein. CB units were tested prior to experiments for their human immune reconstitution potential. Only CB units that resulted in >20% huCD45$^+$ cells in PBL at week 10 post-HCT were used in studies. Cryopreserved and QC iDCtWT1 were thawed and injected into NRG at 7, 8, 11, 12, 15, and 16 weeks post-HCT and for NSG-A2, at 6, 7, 10, 11, 14, and 15 weeks post-HCT. Mice were immunized with a total dose of 1×10^5 iDCtWT1 cells per injection time point and injected s.c. near the anatomical regions of the inguinal and axillary lymph nodes.

Analysis of immune reconstitution by flow cytometry

Cells recovered from the spleen and blood were incubated with a hypotonic solution (0.83% ammonium chloride/20 mM HEPES, pH 7.2, for 5 min at room temperature [RT]) to lyse the erythrocytes. Blood and tissues were further processed for immune staining and flow cytometry analyses as described before.[42] Cells were incubated with PBS containing 10% human serum for blocking (20 min on ice), washed, and incubated with prior titrated antibody concentrations for 30 min on ice. Cells were washed to remove unspecific antibodies. Data were obtained with an LSR II cytometer (BD Biosciences, Franklin Lakes, NJ, USA) and analyzed with FlowJo (Treestar, Ashland, OR, USA). The antibodies used are listed in Table S1.

Analyses of WT1 expression by quantitative real-time PCR

For quantitative real-time PCR analysis of WT1 mRNA expression in cells, RNA was purified using the QIAamp RNeasy Mini Kit (QIAGEN, Hilden, Germany). WT1 RNA quantification was performed according to the kit's manufacturer's instructions using the ipsogen WT1 ProfileQuant Kit CE (QIAGEN, Hilden, Germany) and StepOnePlus Real-Time PCR Detection System (Applied Biosystems, Darmstadt, Germany).

Intracellular cytokine staining

Cryopreserved cell material obtained from spleens or MLNs was thawed and washed once to remove the remaining DMSO. MLNs from each experimental group from the NRG experiment were pooled together for analysis. Subsequently, cells were resuspended in TexMACS medium (Miltenyi Biotec) supplemented with 3% heat-inactivated human serum (c.c.pro, Oberdorla, Germany) and 5 ng/mL IL-7 and IL-15 (Miltenyi Biotec, Bergisch-Gladbach, Germany). $5 \times 10^5 - 1 \times 10^6$ cells were seeded into each well of a 96-well U-bottom plate (Sarstedt, Nümbrecht, Germany). Cells were rested at 37°C and 5% CO$_2$ for 16 h, followed by stimulation with 500 ng/mL of WT1 PepTivator (Miltenyi Biotec, Bergisch-Gladbach, Germany) and 500 ng/mL of WT1$_{126-134}$ peptide (RMFPNAPYL; IBA Lifesciences, Göttingen, Germany). As positive-staining controls, cells were stimulated with 10 ng/mL of phorbol 12-myristate 13-acetate (PMA; Sigma-Aldrich, St. Louis, MO, USA) and 500 ng/mL of ionomycin (Sigma-Aldrich), and unstimulated cells were used as negative controls. After 1 h of stimulation, 5 μg/mL of brefeldin A (BioLegend, San Diego, CA, USA) was added to each well, and cells were carefully mixed by pipetting. Cells were incubated at 37°C and 5% CO$_2$ for a further 4 h. For staining, cells were harvested into 5 mL polystyrene tubes (Sarstedt, Nümbrecht, Germany) and washed once with PBS (Lonza, Basel, Switzerland) prior to surface staining. Afterward, cells were fixed, permeabilized, and stained intracellularly using IntraPrep Permeabilization Reagent (Beckman Coulter, Brea, CA, USA) according to the manufacturer's instructions. The antibodies used are listed in Table S1. Samples were acquired at FACS-Canto with 10-color configuration (BD Biosciences) using FACSDiva 8.0.1 (BD Biosciences) and analyzed with FlowJo (Treestar).

Detection of human cytokines and Igs in plasma

Human Th1/Th2 cytokines in plasma were quantified by a fluorescent magnetic bead-based 14-plex Luminex assay (Merck Millipore, Darmstadt, Germany) and human Ig subtypes by bead-based 6-plex LEGENDplex immunoassay (BioLegend). Human cytokines in cell culture supernatant were quantified by bead-based 6-plex LEGEND-plex immunoassay (BioLegend). Concentrations were determined according to the manufacturer's instructions. Samples were measured in duplicates.

GL manufacturing of iDCtWT1
Instrumentation and tubing set

The GMP-compliant manufacturing of iDCtWT1 was performed using the CliniMACS Prodigy platform (Miltenyi Biotec), which allows an automated cell processing in a closed system controlled by

operating software version (v.)1.3 and process software for TCT v.2.0 (released). The TCT process software was previously designed for the manufacturing of CAR-T cells. Therefore, adaptations were performed in order to adapt processing to allow CD14 selection, pre-conditioning, and transduction. Within the scope of the automatically running process, the input of different variable process parameters, like time points of transduction, media exchange, culture wash, harvesting, and volume of media exchange, was feasible (activity matrix). The installation of CliniMACS Prodigy Tubing Set TS520 and the operational interventions were carried out via the graphical user interface of the Prodigy. Pre-prepared sterile buffer, media, starting cell material, and vector were connected directly to TS520 via a sterile tubing welder device (TSCD II; Terumo Blood and Cell Technologies [BCT]).

Buffer, media, reagents, and culture conditions

Clinical-grade materials for iDCtWT1 cell production were used if available. Detailed information regarding the materials was recorded, including the supplier, lot number, and expiration date. GMP-compliant reagents (Miltenyi Biotec) were used if not otherwise stated. For immunomagnetic selection of CD14$^+$ cells, CliniMACS PBS/EDTA buffer, supplemented with human serum albumin (HSA; 200 g/L; Baxalta, Shire Deutschland, Berlin, Germany) to a final concentration of 0.5% and CliniMACS CD14 reagent, was used. For cytokine stimulation and culturing of cells, the basal medium DendriMACS GMP medium for run 1 or TheraPEAK X-VIVO 15 medium (Lonza) for run 2 was supplemented with 56 ng/mL (616 IU/mL) MACS GMP Recombinant Human GM-CSF and 74 ng/mL (244 IU/mL) MACS GMP Recombinant Human IL-4. During cultivation, the temperature and atmosphere were maintained at 37°C with 5% CO_2. The final product was formulated in Composol PS (Fresenius Kabi AG, Bad Homburg, Germany)/2.86% HSA, and for cryopreservation, the cell suspension was diluted and mixed with DMSO (CryoSure-DMSO, USP grade; WAK Chemie, Steinbach, Germany) to a final concentration of 10% (v/v).

Operational sequence

For a schematic illustration of the manufacturing process, see Figure 5A. Starting material for iDCtWT1 was CD14$^+$ cells derived from non-mobilized leukapheresis material. Cell processing started within 24 h after leukapheresis collection with immunomagnetic enrichment of CD14$^+$ cells. After 6 h of cytokine stimulation, transduction was performed by adding 15 mL LV with a dose of 2.5 × 10^3 ng p24/5 × 10^6 for RG-IDLV or 1.0 × 10^2 ng p24/5 × 10^6 cells for GL-IDLV plus 5 μg/mL protamine sulfate (heparin-antidot 1,400 international units (I.E.)/mL; LEO Pharma, Neu-Isenburg, Germany) and culturing the cells for 16 h. After culture wash and harvest, the cells were automatically formulated in pre-cooled resuspension buffer (Composol PS/2.86% HSA) using the CliniMACS Prodigy device. The cell density was manually adjusted to 4 × 10^6/mL, 10 × 10^6/mL, or 22 × 10^6/mL. For cryopreservation, 1:1 dilutions were performed with same volume of pre-cooled resuspension buffer containing 20% DMSO. 1 mL aliquots of the cell suspensions containing 10% DMSO were dispensed into cryogenic storage vials. The cryovials

were placed in an isopropanol chamber and stored at −80°C overnight and then stored in the vapor phase above liquid nitrogen at <−140°C. Aliquots of 2 × 10^6 cells/mL were used for analysis of cell recovery after freezing and thawing. Aliquots of 5 × 10^6 cells/mL and 11 × 10^6 cells/mL were used for *in vitro* and *in vivo* experiments, respectively.

Flow cytometric characterization of cell product manufactured in the CliniMACS Prodigy

The total cell numbers and cell viabilities were analyzed for samples collected pre- and post-selection, after medium exchange for pre-conditioning, and in the final product before cryopreservation. Flow cytometric analysis was performed for quantification of CD45$^+$ hematopoietic cells, CD14$^+$ monocytes, CD34$^+$ stem cell progenitors, CD3$^+$ T cells, CD19$^+$ B cells, and CD56$^+$ NK cells (the conjugated monoclonal antibodies are listed in Table S1). A maximum of 2 × 10^6 cells were stained with the indicated volume of antibodies (see Table S1). The cells were then stained with 7-AAD for 15 min at RT for discrimination of dead cells. Afterward, the cells were incubated with freshly prepared IOTest3 Lysing Solution (Beckman Coulter) for 15 min at RT according to the manufacturer's instructions. Prior to acquisition analyses by flow cytometry, FlowCount Beads (Beckman Coulter) were added to the samples according to the manufacturer's instructions. Analyses were performed with the Navios flow cytometer (Navios 3L 10C, software 1.3; Beckman Coulter). Cell debris were excluded via forward-scatter (FSC)/side-scatter (SSC) scatterplot. Viable leukocytes were defined as CD45$^+$ and 7-AAD^{neg}. Viable CD45$^+$ leukocytes were further analyzed for the frequencies of CD34$^+$, CD3$^+$, CD19$^+$, CD14$^+$, and CD56$^+$ cells (see gating strategy in Figure S7A).

Thawing and culturing of iDCtWT1 after manufacturing in the CliniMACS Prodigy

For analysis of recovery after cryopreservation, cells were thawed in a 37°C water bath and stained with trypan blue, and viable cells were counted using a Neubauer chamber. For characterization of iDCtWT1 differentiation, cells were thawed in a 37°C water bath, washed in 50 mL of PBS, and resuspended in a density of 1 × 10^6 cells/mL in DendriMACS GMP medium (for RG) or TheraPEAK X-VIVO 15 medium (for GL). Cells were cultured in the absence of exogenous cytokines for 7 days at 37°C 5% CO_2. Cells were then harvested for flow cytometric analyses for quantification of viable DCs (the antibodies used are listed in Table S1; 7-AAD staining was performed as above). After setting the gate on live cells (7-AAD^{neg} population), CD45$^+$/CD11c^{bright} were gated for analyses of HLA-DR$^+$/CD86$^+$ and HLA-DR$^+$/CD83$^+$ DCs. For exemplary gating, see Figure S7B.

Histopathological analysis

For histopathological analysis and immunohistochemistry, tissues were fixed in 4% buffered formaldehyde solution for 24 h and embedded in paraffin. Slides of 3 μm thickness were cut from the paraffin block and stained with hematoxylin and eosin, or immunohistochemistry was performed. For the detection of human cells, a

monoclonal mouse AHN antibody (MAB4383; Merck Millipore; dilution 1:100); for CD4, a monoclonal rabbit anti-huCD4 (ab133616; Abcam, Berlin, Germany; dilution 1:100); and for CD8, a monoclonal mouse anti-huCD8 (ab17147; Abcam; dilution 1:25) were used.

Statistical analysis

Data were collected as absolute cell counts from human lymphocyte subsets and expressed in the percent range for both blood and tissues (number of positive cells and percent positive cells). Data were organized in a PivotTable using Excel software 2010 (Microsoft, Redmond, WA, USA). ANOVA and Šidák post hoc tests were applied for comparisons of longitudinal data between groups. Negative binomial regression was used for the comparison of total cell counts. The regression was calculated in the open-source statistics software R (R Core Team 2018) using the *glm.bn* function from the MASS package. Results were expressed as rate ratios. Unpaired t tests of log-transformed data using the Holm-Šidák method for multiplicity adjustment were used for the analysis of the cytokine and Ig concentrations in plasma. Statistical analyses were performed using GraphPad Prism v.7 software (GraphPad Software, La Jolla, CA, USA).

SUPPLEMENTAL INFORMATION

Supplemental information can be found online at https://doi.org/10.1016/j.omtm.2021.04.004.

AUTHOR CONTRIBUTIONS

J.K.B.-W. co-coordinated and managed the project, planned and performed experiments, analyzed data, wrote the first draft of the manuscript, and edited the final manuscript. S.D. and F.F. produced and tested the GL vector. R.E., W.G., M.M., K.A., L.A., and U.K. developed the process for automated cell manufacturing and QC for batch release. S.K., A.S., J.K., S.J.T., H.-C.T., A.D.A.C., and C.F. performed experiments and analyzed data. A.B. and B.E.-V. planned and executed assays to detect WT1-specific responses. D.S. performed the histopathology and immunohistochemistry analysis. S.R.T. and L.M.S. revised or conducted the statistical analyses. C.v.K. provided cord blood, R.B. provided leukapheresis, and C.C. provided technical assistance for adaptation of the manufacturing protocol for the Prodigy. A.B. assisted with the mouse breeding. M.H. assisted with the development of the mouse study protocol. M.H. and A.G. provided clinical input for the discussion with the regulatory agency. R.S. planned and managed the project with the collaborating consortium, provided overall conceptualization and project leadership, obtained funding, supervised the data analyses, and wrote and revised the final manuscript.

DECLARATION OF INTERESTS

R.S. and A.G. are co-inventors in the US- and EU-granted patent "Induced Dendritic Cells and Uses Thereof," publication number WO/2014/122035; PCT/EP2014/051422 (in national phases in China, Japan, and Canada). R.S. received honoraria and research funding from The Jackson Laboratory, a not-for-profit organization developing and commercializing humanized mouse models.

REFERENCES

1. Döhner, H., Estey, E., Grimwade, D., Amadori, S., Appelbaum, F.R., Büchner, T., Dombret, H., Ebert, B.L., Fenaux, P., Larson, R.A., et al. (2017). Diagnosis and management of AML in adults: 2017 ELN recommendations from an international expert panel. Blood *129*, 424–447.

2. Heuser, M., Ofran, Y., Boissel, N., Brunet Mauri, S., Craddock, C., Janssen, J., Wierzbowska, A., and Buske, C.; ESMO Guidelines Committee. Electronic address: (2020). Acute myeloid leukaemia in adult patients: ESMO Clinical Practice Guidelines for diagnosis, treatment and follow-up. Ann. Oncol. *31*, 697–712, clinicalguidelines@esmo.org.

3. Ivey, A., Hills, R.K., Simpson, M.A., Jovanovic, J.V., Gilkes, A., Grech, A., Patel, Y., Bhudia, N., Farah, H., Mason, J., et al.; UK National Cancer Research Institute AML Working Group (2016). Assessment of Minimal Residual Disease in Standard-Risk AML. N. Engl. J. Med. *374*, 422–433.

4. Thol, F., Gabdoulline, R., Liebich, A., Klement, P., Schiller, J., Kandziora, C., Hambach, L., Stadler, M., Koenecke, C., Flintrop, M., et al. (2018). Measurable residual disease monitoring by NGS before allogeneic hematopoietic cell transplantation in AML. Blood *132*, 1703–1713.

5. Kolb, H.J., and Schmid, C. (2020). The FLAMSA concept-past and future. Ann. Hematol. *99*, 1979–1988.

6. Dholaria, B., Savani, B.N., Hamilton, B.K., Oran, B., Liu, H.D., Tallman, M.S., Ciurea, S.O., Holtzman, N.G., Ii, G.L.P., Devine, S.M., et al. (2021). Hematopoietic Cell Transplantation in the Treatment of Newly Diagnosed Adult Acute Myeloid Leukemia: An Evidence-Based Review from the American Society of Transplantation and Cellular Therapy. Transplant Cell Ther *27*, 6–20.

7. D'Souza, A., Fretham, C., Lee, S.J., Arora, M., Brunner, J., Chhabra, S., Devine, S., Eapen, M., Hamadani, M., Hari, P., et al. (2020). Current Use of and Trends in Hematopoietic Cell Transplantation in the United States. Biol. Blood Marrow Transplant. *26*, e177–e182.

8. Daenthanasanmak, A., Salguero, G., Borchers, S., Figueiredo, C., Jacobs, R., Sundarasetty, B.S., Schneider, A., Schambach, A., Eiz-Vesper, B., Blasczyk, R., et al. (2012). Integrase-defective lentiviral vectors encoding cytokines induce differentiation of human dendritic cells and stimulate multivalent immune responses in vitro and in vivo. Vaccine *30*, 5118–5131.

9. Daenthanasanmak, A., Salguero, G., Sundarasetty, B.S., Waskow, C., Cosgun, K.N., Guzman, C.A., Riese, P., Gerasch, L., Schneider, A., Ingendoh, A., et al. (2015). Engineered dendritic cells from cord blood and adult blood accelerate effector

T cell immune reconstitution against HCMV. Mol. Ther. Methods Clin. Dev. *1*, 14060.

10. Sundarasetty, B.S., Singh, V.K., Salguero, G., Geffers, R., Rickmann, M., Macke, L., Borchers, S., Figueiredo, C., Schambach, A., Gullberg, U., et al. (2013). Lentivirus-induced dendritic cells for immunization against high-risk WT1(+) acute myeloid leukemia. Hum. Gene Ther. *24*, 220–237.

11. Sundarasetty, B.S., Kloess, S., Oberschmidt, O., Naundorf, S., Kuehlcke, K., Daenthanasanmak, A., Gerasch, L., Figueiredo, C., Blaszczyk, R., Ruggiero, E., et al. (2015). Generation of lentivirus-induced dendritic cells under GMP-compliant conditions for adaptive immune reconstitution against cytomegalovirus after stem cell transplantation. J. Transl. Med. *13*, 240.

12. Stripecke, R., Münz, C., Schuringa, J.J., Bissig, K.D., Soper, B., Meeham, T., Yao, L.C., Di Santo, J.P., Brehm, M., Rodriguez, E., et al. (2020). Innovations, challenges, and minimal information for standardization of humanized mice. EMBO Mol. Med. *12*, e8662.

13. Volk, V., Reppas, A.I., Robert, P.A., Spineli, L.M., Sundarasetty, B.S., Theobald, S.J., Schneider, A., Gerasch, L., Deves Roth, C., Klöss, S., et al. (2017). Multidimensional Analysis Integrating Human T-Cell Signatures in Lymphatic Tissues with Sex of Humanized Mice for Prediction of Responses after Dendritic Cell Immunization. Front. Immunol. *8*, 1709.

14. Theobald, S.J., Kreer, C., Khailaie, S., Bonifacius, A., Eiz-Vesper, B., Figueiredo, C., Mach, M., Backovic, M., Ballmaier, M., Koenig, J., et al. (2020). Repertoire characterization and validation of gB-specific human IgGs directly cloned from humanized mice vaccinated with dendritic cells and protected against HCMV. PLoS Pathog. *16*, e1008560.

15. Sundarasetty, B., Volk, V., Theobald, S.J., Rittinghausen, S., Schaudien, D., Neuhaus, V., Figueiredo, C., Schneider, A., Gerasch, L., Mucci, A., et al. (2017). Human Effector Memory T Helper Cells Engage with Mouse Macrophages and Cause Graft-versus-Host-Like Pathology in Skin of Humanized Mice Used in a Nonclinical Immunization Study. Am. J. Pathol. *187*, 1380–1398.

16. Merli, P., Caruana, I., De Vito, R., Strocchio, L., Weber, G., Bufalo, F.D., Buatois, V., Montanari, P., Cefalo, M.G., Pitisci, A., et al. (2019). Role of interferon-γ in immune-mediated graft failure after allogeneic hematopoietic stem cell transplantation. Haematologica *104*, 2314–2323.

17. Najima, Y., Tomizawa-Murasawa, M., Saito, Y., Watanabe, T., Ono, R., Ochi, T., Suzuki, N., Fujiwara, H., Ohara, O., Shultz, L.D., et al. (2016). Induction of WT1-specific human CD8+ T cells from human HSCs in HLA class I Tg NOD/SCID/IL2rgKO mice. Blood *127*, 722–734.

18. Aleksandrova, K., Leise, J., Priesner, C., Melk, A., Kubaink, F., Abken, H., Hombach, A., Aktas, M., Essl, M., Bürger, I., et al. (2019). Functionality and Cell Senescence of CD4/CD8-Selected CD20 CAR T Cells Manufactured Using the Automated CliniMACS Prodigy® Platform. Transfus. Med. Hemother. *46*, 47–54.

19. Przespolewski, A.C., and Griffiths, E.A. (2020). BITES and CARS and checkpoints, oh my! Updates regarding immunotherapy for myeloid malignancies from the 2018 annual ASH meeting. Blood Rev. *43*, 100654.

20. Inoue, K., Sugiyama, H., Ogawa, H., Nakagawa, M., Yamagami, T., Miwa, H., Kita, K., Hiraoka, A., Masaoka, T., Nasu, K., et al. (1994). WT1 as a new prognostic factor and a new marker for the detection of minimal residual disease in acute leukemia. Blood *84*, 3071–3079.

21. Ogawa, H., Tamaki, H., Ikegame, K., Soma, T., Kawakami, M., Tsuboi, A., Kim, E.H., Hosen, N., Murakami, M., Fujioka, T., et al. (2003). The usefulness of monitoring WT1 gene transcripts for the prediction and management of relapse following allogeneic stem cell transplantation in acute type leukemia. Blood *101*, 1698–1704.

22. Di Stasi, A., Jimenez, A.M., Minagawa, K., Al-Obaidi, M., and Rezvani, K. (2015). Review of the Results of WT1 Peptide Vaccination Strategies for Myelodysplastic Syndromes and Acute Myeloid Leukemia from Nine Different Studies. Front. Immunol. *6*, 36.

23. Talarn, C., Urbano-Ispizua, A., Martino, R., Pérez-Simón, J.A., Batlle, M., Herrera, C., Granell, M., Gaya, A., Torrebadell, M., Fernández-Avilés, F., et al. (2007). Kinetics of recovery of dendritic cell subsets after reduced-intensity conditioning allogeneic stem cell transplantation and clinical outcome. Haematologica *92*, 1655–1663.

24. Rickmann, M., Macke, L., Sundarasetty, B.S., Stamer, K., Figueiredo, C., Blaszczyk, R., Heuser, M., Krauter, J., Ganser, A., and Stripecke, R. (2013). Monitoring dendritic cell and cytokine biomarkers during remission prior to relapse in patients with FLT3-ITD acute myeloid leukemia. Ann. Hematol. *92*, 1079–1090.

25. Saxena, M., and Bhardwaj, N. (2017). Turbocharging vaccines: emerging adjuvants for dendritic cell based therapeutic cancer vaccines. Curr. Opin. Immunol. *47*, 35–43.

26. Van Tendeloo, V.F., Van de Velde, A., Van Driessche, A., Cools, N., Anguille, S., Ladell, K., Gostick, E., Vermeulen, K., Pieters, K., Nijs, G., et al. (2010). Induction of complete and molecular remissions in acute myeloid leukemia by Wilms' tumor 1 antigen-targeted dendritic cell vaccination. Proc. Natl. Acad. Sci. USA *107*, 13824–13829.

27. Lichtenegger, F.S., Schnorfeil, F.M., Rothe, M., Deiser, K., Altmann, T., Bücklein, V.L., Köhnke, T., Augsberger, C., Konstandin, N.P., Spiekermann, K., et al. (2020). Toll-like receptor 7/8-matured RNA-transduced dendritic cells as post-remission therapy in acute myeloid leukaemia: results of a phase I trial. Clin. Transl. Immunology *9*, e1117.

28. Bialek-Waldmann, J.K., Heuser, M., Ganser, A., and Stripecke, R. (2019). Monocytes reprogrammed with lentiviral vectors co-expressing GM-CSF, IFN-α2 and antigens for personalized immune therapy of acute leukemia pre- or post-stem cell transplantation. Cancer Immunol. Immunother. *68*, 1891–1899.

29. Mo, X., Zhang, X., Xu, L., Wang, Y., Yan, C., Chen, H., Chen, Y., Han, W., Wang, F., Wang, J., et al. (2019). Interferon-α salvage treatment is effective for patients with acute leukemia/myelodysplastic syndrome with unsatisfactory response to minimal residual disease-directed donor lymphocyte infusion after allogeneic hematopoietic stem cell transplantation. Front. Med. *13*, 238–249.

30. Kolb, H.J., Rank, A., Chen, X., Woiciechowsky, A., Roskrow, M., Schmid, C., Tischer, J., and Ledderose, G. (2004). In-vivo generation of leukaemia-derived dendritic cells. Best Pract. Res. Clin. Haematol. *17*, 439–451.

31. Escobar, G., Barbarossa, L., Barbiera, G., Norelli, M., Genua, M., Ranghetti, A., Plati, T., Camisa, B., Brombin, C., Cittaro, D., et al. (2018). Interferon gene therapy reprograms the leukemia microenvironment inducing protective immunity to multiple tumor antigens. Nat. Commun. *9*, 2896.

32. Lapenta, C., Gabriele, L., and Santini, S.M. (2020). IFN-Alpha-Mediated Differentiation of Dendritic Cells for Cancer Immunotherapy: Advances and Perspectives. Vaccines (Basel) *8*, 617.

33. Ho, V.T., and Soiffer, R.J. (2001). The history and future of T-cell depletion as graft-versus-host disease prophylaxis for allogeneic hematopoietic stem cell transplantation. Blood *98*, 3192–3204.

34. Schmied, S., Gostick, E., Price, D.A., Abken, H., Assenmacher, M., and Richter, A. (2015). Analysis of the functional WT1-specific T-cell repertoire in healthy donors reveals a discrepancy between CD4(+) and CD8(+) memory formation. Immunology *145*, 558–569.

35. Mendoza, M., Gunasekera, D., Pratt, K.P., Qiu, Q., Casares, S., and Brumeanu, T.D. (2020). The humanized DRAGA mouse (HLA-A2. HLA-DR4. RAG1 KO. IL-2R g c KO. NOD) establishes inducible and transmissible models for influenza type A infections. Hum. Vaccin. Immunother. *16*, 2222–2237.

36. Williams, B.A., Law, A., Hunyadkurti, J., Desilets, S., Leyton, J.V., and Keating, A. (2019). Antibody Therapies for Acute Myeloid Leukemia: Unconjugated, Toxin-Conjugated, Radio-Conjugated and Multivalent Formats. J. Clin. Med. *8*, 1261.

37. Balar, A.V., and Weber, J.S. (2017). PD-1 and PD-L1 antibodies in cancer: current status and future directions. Cancer Immunol. Immunother. *66*, 551–564.

38. June, C.H., O'Connor, R.S., Kawalekar, O.U., Ghassemi, S., and Milone, M.C. (2018). CAR T cell immunotherapy for human cancer. Science *359*, 1361–1365.

39. Anguille, S., Van de Velde, A.L., Smits, E.L., Van Tendeloo, V.F., Juliusson, G., Cools, N., Nijs, G., Stein, B., Lion, E., Van Driessche, A., et al. (2017). Dendritic cell vaccination as postremission treatment to prevent or delay relapse in acute myeloid leukemia. Blood *130*, 1713–1721.

40. Godbey, W.T., Wu, K.K., and Mikos, A.G. (1999). Poly(ethylenimine) and its role in gene delivery. J. Control. Release *60*, 149–160.

41. Sundarasetty, B.S., Chan, L., Darling, D., Giunti, G., Farzaneh, F., Schenck, F., Naundorf, S., Kuehlcke, K., Ruggiero, E., Schmidt, M., et al. (2015). Lentivirus-induced 'Smart' dendritic cells: Pharmacodynamics and GMP-compliant production for immunotherapy against TRP2-positive melanoma. Gene Ther. *22*, 707–720.

42. Salguero, G., Daenthanasanmak, A., Münz, C., Raykova, A., Guzmán, C.A., Riese, P., Figueiredo, C., Länger, F., Schneider, A., Macke, L., et al. (2014). Dendritic cell-mediated immune humanization of mice: implications for allogeneic and xenogeneic stem cell transplantation. J. Immunol. *192*, 4636–4647.

43. Maetzig, T., Kuehle, J., Schwarzer, A., Turan, S., Rothe, M., Chaturvedi, A., Morgan, M., Ha, T.C., Heuser, M., Hammerschmidt, W., et al. (2014). All-in-One inducible lentiviral vector systems based on drug controlled FLP recombinase. Biomaterials *35*, 4345–4356.

44. Bustin, S.A., Benes, V., Garson, J.A., Hellemans, J., Huggett, J., Kubista, M., Mueller, R., Nolan, T., Pfaffl, M.W., Shipley, G.L., et al. (2009). The MIQE guidelines: minimum information for publication of quantitative real-time PCR experiments. Clin. Chem. *55*, 611–622.